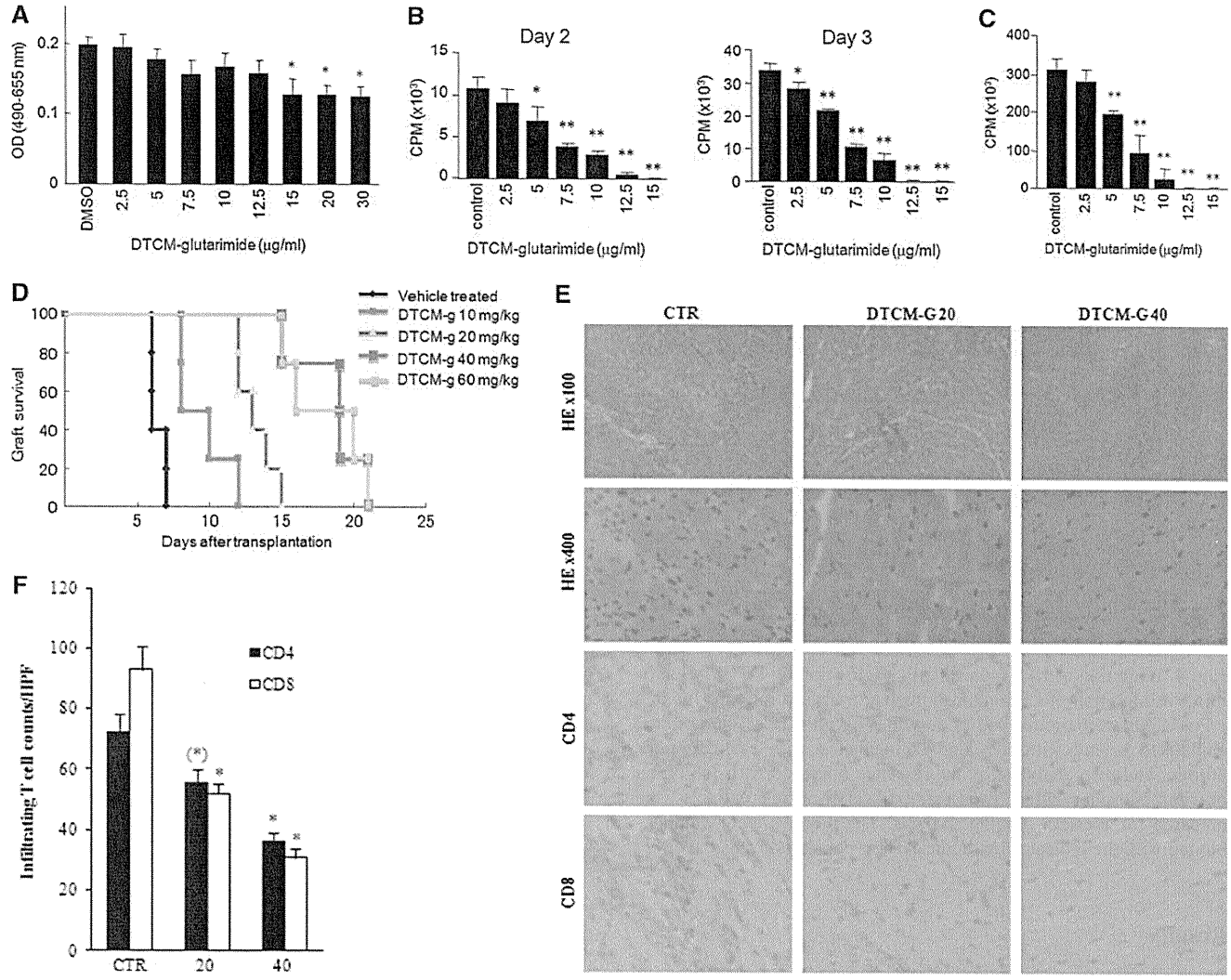

Fig. 5 Inhibition of mixed lymphocyte reaction and of graft rejection by DTCM-glutarimide. **a** Cytotoxicity of DTCM-glutarimide toward the responder C57BL/6 spleen cells. DTCM-glutarimide was added to the cells, which were then incubated for 6 h, after which the viability was assessed by performing the MTT assay. Values are the means and SD of three determinations. $*P < 0.05$. **b** Inhibition of the mixed lymphocyte reaction by mouse spleen cells. The responder C57BL/6 and stimulating BALB/c cells were co-cultured for 48 or 72 h. MLR was assessed by thymidine incorporation. Values are the means and SD of three or four determinations. $*P < 0.05$, $**P < 0.005$. **c** Inhibition of proliferation of purified T cells. Purified C57BL/6 T cells were stimulated with 1 μg/ml CD28 in plates precoated with anti-CD3 in the presence of DTCM-glutarimide for 48 h. The proliferation was measured by thymidine incorporation. Each value is the mean and SD of four4 determinations. $*P < 0.005$. **d** Inhibition of graft rejection by DTCM-glutarimide in mouse heart transplantation. As in the case of the donor/recipient strains of cells used in the MLR, the hearts of BALB/c (H-2d) mice were transplanted into C57BL/6 (H-2b) mice. DTCM-glutarimide at 10–60 mg/kg was given intraperitoneally every day from just before the transplantation. **e** Histology of cardiac grafts following transplantation. Cardiac allografts were stained with H&E (original magnification: ×100 or ×400), anti-CD4 (×400), or anti-CD8 Abs (×400). Representative photographs of four independent grafts on day 5 are shown. **f** The numbers of $CD4^+$ and $CD8^+$ cells in graft sections were counted in three different high power fields (HPF) and then quantified. Each bar represents the mean ± SEM of four independent experiments. $*P < 0.05$ versus control. (*CTR* control)

concentrations. On the other hand, it had no effect on the activation of MAPKs including p38, ERK, and JNK (Fig. 4c), so we expect that DTCM-glutarimide would inhibit the kinase activity of JNK. But it did not inhibit the phosphorylation of c-Jun by JNK in vitro (Fig. 4d). Thus, it is likely that DTCM-glutarimide would inhibit AP-1 activation by inhibition of the cofactors for JNK.

Inhibition of mixed lymphocyte reaction by DTCM-glutarimide

The mixed lymphocyte reaction (MLR) is known to be positively regulated by AP-1 [14, 15]. We employed spleen cells from C57BL/6 mice as responder cells and irradiated spleen cells from BALB/c mice as the stimulating cells.

Table 1 Amelioration of mouse cardiac allograft survival by DTCM-glutarimide treatment

DTCM-glutarimide (mg/kg)	N	Survival (days)	Median survival (days)
0	6	6, 6, 6, 6, 7, 7	6.0
10	4	8, 8, 10, 12	9.0#
20	4	12, 13, 14, 15	13.5#
40	4	15, 19, 19, 21	19.0#
60	4	15, 16, 20, 21	18.0#

# $P < 0.05$ versus control

When C57BL/6 spleen cells were incubated with DTCM-glutarimide for 6 h, their viability was not affected even at 12.5 μg/ml, as assessed by MTT analysis (Fig. 5a). The responder and stimulating cells were co-cultured for 48 or 72 h. DTCM-glutarimide at 5–12.5 μg/ml inhibited the MLR assessed by thymidine incorporation (Fig. 5b). As the MLR is dependent on responder T cell proliferation, we measured the effect of DTCM-glutarimide on the proliferation of C57BL/6 T cells purified by use of an enrichment column. The cells were then stimulated with anti-CD28 and anti-CD3 for 48 h. As shown in Fig. 5c, at concentrations of 5 μg/ml and above, DTCM-glutarimide inhibited the proliferation.

Inhibition of graft rejection by DTCM-glutarimide in mouse heart transplantation

The hearts of BALB/c (H-2d) mice were transplanted to C57BL/6 (H-2b) mice. DTCM-glutarimide at 10–60 mg/kg was given intraperitoneally every day from just before the transplantation. As shown in Fig. 5d and Table 1, at 10–40 mg/kg the analog prolonged the graft survival dose dependently. The effect appeared to be saturated at 40 mg/kg, and no toxicity was observed during the experiment even at 60 mg/kg. We also looked into the histology of cardiac sections. As shown in Fig. 5e and f, the numbers of CD4-positive and CD8-positive cells were reduced by the treatment of 20 or 40 mg/kg DTCM-glutarimide.

Discussion

The free radical NO produced by eNOS often plays an important role in regulating many physiological functions such as vasodilation and neurotransmission. However, overproduction of NO by iNOS in macrophages often provokes inflammatory diseases including atherosclerosis, rheumatoid arthritis, diabetes, septic shock, transplant rejection, and multiple sclerosis. Therefore, suppression of iNOS expression might be important for the treatment of inflammatory disorders [16, 17]. Since DTCM-glutarimide inhibits the expression of iNOS, it would be a possible candidate for use as an anti-inflammatory agent. Cyclooxygenase (COX) is a key enzyme catalyzing the rate-limiting step in the biosynthesis of prostaglandins from arachidonic acid [18, 19]. COX-2 often plays a key role in inflammation and also tumorigenesis [20, 21]. Because DTCM-glutarimide lowered the COX-2 expression (Fig. 2c), it may be a potential drug for treating inflammatory and neoplastic diseases.

Being a 9-methylstreptimidone derivative, DTCM-glutarimide inhibited the expression of iNOS and COX-2; but, unexpectedly, it did not inhibit the LPS-induced IL-6 secretion and NF-κB activation at all, unlike the NF-κB inhibitor (−)-DHMEQ (Fig. 3a–c). Next, we examined the effect of DTCM-glutarimide on the activation of AP-1, because the promoter regions of both the iNOS and COX-2 genes contain the binding sites for NF-κB and AP-1 [22, 23]. As shown in Fig. 4a–b, DTCM-glutarimide inhibited AP-1 activation at concentrations that inhibited NO production and the expression of iNOS and COX-2.

AP-1 is a heterodimer consisting of a member of the Jun family proteins and one of the Fos or ATF family proteins. A Jun/Jun homodimer is also possible [24]. The Jun family proteins include c-Jun, JunB, and JunD [24]; the Fos family ones, c-Fos, FosB, Fra-1, and Fra-2 [25–28]; and the ATF family ones, ATF-2, ATF-3/LRF1, and B-ATF [29–31]. Each AP-1 protein is phosphorylated in the cytoplasm, and enters the nucleus to form the dimer. The Jun/Fos complex mainly binds to the TPA-responsive element (TRE); and the Jun/ATF complex, to the cyclic AMP-responsive element (CRE; 24, 28). The c-Jun/c-Fos heterodimer is the most common form of AP-1.

Activation of JNK leads to the phosphorylation of c-Jun and an increase in the transcriptional activity of AP-1 [32]. Our finding that DTCM-glutarimide inhibited the cellular phosphorylation of c-Jun (Fig. 4b) indicates that the inhibition of AP-1 activation by this compound would be due to inhibition upstream of the c-Jun phosphorylation. We demonstrated that DTCM-glutarimide did not affect the activation of various MAPKs (Fig. 4c), and also did not inhibit the phosphorylation of recombinant c-Jun by recombinant JNK (Fig. 4d). Therefore, it is possible that DTCM-glutarimide would inhibit the cofactor activity of JNK. The effect of DTCM-glutarimide on AP-1 components other than c-Jun and the molecular target remain to be studied.

DTCM-glutarimide inhibited the MLR reaction and purified T-cell proliferation. Also, in the in vivo study, it increased the graft survival time of transplanted hearts in mice. The effective dose of DTCM-glutarimide at 10–60 mg/kg did not show any toxicity. Thus, DTCM-glutarimide may be stable in the animal body and

distributed widely to the organs. Histological observation indicated that treatment with DTCM-glutarimide lowers the number of CD4- and CD8-positive cells in the cardiac section. The mechanism of MLR inhibition and graft survival may also include some activity of DTCM-glutarimide other than AP-1 inhibition.

A small molecular weight AP-1 inhibitor, T-5224, was designed to interact with AP-1 proteins, and it inhibits rheumatoid arthritis in animals [33]. Compared with T-5224, DTCM-glutarimide is likely to inhibit AP-1 functions by a different mechanism. Moreover, having a simpler structure, it may be more advantageous than T-5224, because DTCM-glutarimide is more easily prepared.

In conclusion, DTCM-glutarimide inhibited the expression of iNOS and COX-2 in a mouse macrophage cell line RAW264.7. The effect may have been partly due to the inhibition of AP-1 activity. Furthermore, it extended the survival time of transplanted hearts in mice. Although the precise mechanism of its anti-inflammatory activity requires further studies, DTCM-glutarimide may be a new candidate as an anti-inflammatory agent.

Acknowledgments This work was financially supported in part by grants from the program Grants-in-Aid for Scientific Research on Priority Areas of the Ministry of Education, Culture, Sports, Science, and Technology (MEXT). It was also supported by a High-Tech Research Center Project for Private Universities: matching fund subsidy from MEXT, 2006–2011, and the Global Center of Excellence Program from MEXT, 2007–2012.

References

1. Matsumoto N, Ariga A, To-e S, Nakamura H, Agata N, Hirano S, et al. Synthesis of NF-kappaB activation inhibitors derived from epoxyquino- micin C. Bioorg Med Chem Lett. 2000;10:865–9.
2. Ariga A, Namekawa J, Matsumoto N, Inoue J, Umezawa K. Inhibition of tumor necrosis f actor-alpha-induced nuclear translocation and activation of NF-kappa B by dehydroxymethylepoxyquinomicin. J Biol Chem. 2002;277:24625–30.
3. Yamamoto M, Horie R, Takeiri M, Kozawa I, Umezawa K. Inactivation of NF-kappaB components by covalent binding of (−)-dehydroxymethylepoxyquinomicin to specific cysteine residues. J Med Chem. 2008;51:5780–8.
4. Watanabe M, Ohsugi T, Shoda M, Ishida T, Aizawa S, Maruyama-Nagai M, Utsunomiya A, Koga S, Yamada Y, Kamihira S, Okayama A, Kikuchi H, Uozumi K, Yamaguchi K, Higashihara M, Umezawa K, Watanabe T, Horie R. Dual targeting of transformed and untransformed HTLV-1-infected T-cells by DHMEQ, a potent and selective inhibitor of NF-κB, as a strategy for chemoprevention and therapy of adult T cell leukemia. Blood. 2005;106:2462–71.
5. Umezawa K. Inhibition of tumor growth by NF-κB inhibitors. Cancer Sci. 2006;97:990–5.
6. Hamasaka A, Yoshioka N, Abe R, Kishino S, Umezawa K, Ozaki M, Todo S, Shimizu H. Topical application of DHMEQ improves allergic inflammation via NF-κB inhibition. J Allergy Clin Immunol. 2010;126:400–3.
7. Ueki S, Yamashita K, Aoyagi T, Haga S, Suzuki T, Itoh T, et al. Control of allograft rejection by applying a novel nuclear factor-kappaB inhibitor, dehydroxymethylepoxy-quinomicin. Transplantation. 2006;82:1720–7.
8. Umezawa K. Screening of bioactive metabolites that suppress inflammation. Tanpakushitsu Kakusan Koso. 2007;52:1685–9.
9. Ishikawa Y, Tachibana M, Matsui C, Obata R, Umezawa K, Nishiyama S. Synthesis and biological evaluation on novel analogs of 9-methylstreptimidone, an inhibitor of NF-kappaB. Bioorg Med Chem Lett. 2009;19:1726–8.
10. Dignam JD, Lebovitz RM, Roeder RG. Accurate transcription initiation by RNA polymerase II in a soluble extract from isolated mammalian nuclei. Nucleic Acids Res. 1983;11:1475–89.
11. Corry RJ, Winn HJ, Russel PS. Primarily vascularized allografts of hearts in mice. The role of H-2D, H-2K, and non-H-2 antigens in rejection. Transplantation. 1973;16:343–50.
12. Nomura M, Yamashita K, Murakami M, Takehara M, Echizenya H, Sunahara M, et al. Induction of donor-specific tolerance by adenovirus-mediated CD40Ig gene therapy in rat liver transplantation. Transplantation. 2002;73(9):1403–10.
13. Jang JH, Surh YJ. AP-1 mediates beta-amyloid-induced iNOS expression in PC12 cells via the ERK2 and p38 MAPK signaling pathways. Biochem Biophys Res Commun. 2005;331:1421–8.
14. Yea SS, Jeong HS, Choi CY, Park KR, Oh S, Shin JG, et al. Inhibitory effect of anethole on T-lymphocyte proliferation and interleukin-2 production through down-regulation of the NF-AT and AP-1. Toxicol In Vitro. 2006;20:1098–105.
15. Thornton TM, Zullo AJ, Williams KL, Taparowsky EJ. Direct manipulation of activator protein-1 controls thymocyte proliferation in vitro. Eur J Immunol. 2006;36:160–9.
16. Park PH, Kim HS, Jin XY, Jin F, Hur J, Ko G, et al. KB-34, a newly synthesized chalcone derivative, inhibits lipopolysaccharide-stimulated nitric oxide production in RAW 264.7 macrophages via heme oxygenase-1 induction and blockade of activator protein-1. Eur J Pharmacol. 2009;606:215–24.
17. Chen CY, Peng WH, Tsai KD, Hsu SL. Luteolin suppresses inflammation-associated gene expression by blocking NF-kappaB and AP-1 activation pathway in mouse alveolar macrophages. Life Sci. 2007;81:1602–14.
18. Smith WL, Garavito RM, DeWitt DL. Prostaglandin endoperoxide H synthases (cyclooxygenases)-1 and -2. J Biol Chem. 1996;271:33157–60.
19. Herschman HR. Prostaglandin synthase 2. Biochim Biophys Acta. 1996;1299:125–40.
20. Vane JR, Bakhle YS, Botting RM. Cyclooxygenases 1 and 2. Annu Rev Pharmacol Toxicol. 1998;38:97–120.
21. Dubois RN, Abramson SB, Crofford L, Gupta RA, Simon LS, Van De Putte LB, et al. Cyclooxygenase in biology and disease. FASEB J. 1998;12:1063–73.
22. Lowenstein CJ, Alley EW, Raval P, Snowman AM, Snyder SH, Russell SW, et al. Macrophage nitric oxide synthase gene: two upstream regions mediate induction by interferon gamma and lipopolysaccharide. Proc Natl Acad Sci USA. 1993;90:9730–4.
23. Yao J, Mackman N, Edgington TS, Fan ST. Inhibitory effect of 1,8-cineol (eucalyptol) on Egr-1 expression in lipopolysaccharide-stimulated THP-1 cells. J Biol Chem. 1997;272:17795–801.
24. Nakabeppu Y, Ryder K, Nathans D. DNA binding activities of three murine Jun proteins: stimulation by Fos. Cell. 1988;5:907–15.
25. Ryseck RP, Kovary K, Bravo R. Integrity of FOS B leucine zipper is essential for its interaction with JUN proteins. Oncogene. 1990;5:1091–3.
26. Cohen DR, Curran T. fra-1: a serum-inducible, cellular immediate-early gene that encodes a fos-related antigen. Mol Cell Biol. 1988;8:2063–9.

27. Nishina H, Sato H, Suzuki T, Sato M, Iba H. Isolation and characterization of fra-2, an additional member of the fos gene family. Proc Natl Acad Sci USA. 1990;87:3619–23.
28. Chiu R, Boyle WJ, Meek J, Smeal T, Hunter T, Karin M. The c-Fos protein interacts with c-Jun/AP-1 to stimulate transcription of AP-1 responsive genes. Cell. 1988;54:541–52.
29. Macgregor PF, Abate C, Curran T. Direct cloning of leucine zipper proteins: Jun binds cooperatively to the CRE with CRE-BP1. Oncogene. 1990;5:451–8.
30. Hsu JC, Laz T, Mohn KL, Taub R. Identification of LRF-1, a leucine-zipper protein that is rapidly and highly induced in regenerating liver. Proc Natl Acad Sci USA. 1991;88:3511–5.
31. Dorsey MJ, Tae HJ, Sollenberger KG, Mascarenhas NT, Johansen LM, Taparowsky EJ. B-ATF: a novel human bZIP protein that associates with members of the AP-1 transcription factor family. Oncogene. 1995;11:2255–65.
32. Dérijard B, Hibi M, Wu IH, Barrett T, Su B, Deng T, Karin M, Davis RJ. JNK1: a protein kinase stimulated by UV light and Ha-Ras that binds and phosphorylates the c-Jun activation domain. Cell. 1994;76:1025–37.
33. Aikawa Y, Morimoto K, Yamamoto T, Chaki H, Hashiramoto A, Narita H, Hirono S, Shiozawa S. Treatment of arthritis with a selective inhibitor of c-Fos/activator protein-1. Nat Biotechnol. 2008;26:817–23.

Cancer Science
The official journal of the Japanese Cancer Association JCA

Inhibition of nuclear factor-kappaB suppresses peritoneal dissemination of gastric cancer by blocking cancer cell adhesion

Kazuhiro Mino,[1] Michitaka Ozaki,[2,7] Kazuaki Nakanishi,[1] Sanae Haga,[2,3] Masanori Sato,[1] Masaya Kina,[1] Masato Takahashi,[1] Norihiko Takahashi,[1] Akihiko Kataoka,[1] Kazuyoshi Yanagihara,[4] Takahiro Ochiya,[5] Toshiya Kamiyama,[1] Kazuo Umezawa[6] and Satoru Todo[1]

[1]Department of General Surgery, Graduate School of Medicine, Hokkaido University, Sapporo; [2]Department of Molecular Surgery, Hokkaido University School of Medicine, Sapporo; [3]The Japan Society for the Promotion of Science (JSPS), Tokyo; [4]Department of Life Sciences, Yasuda Women's University Faculty of Pharmacy, Hiroshima; [5]Section for Studies on Metastasis, National Cancer Center Research Institute, Tokyo; [6]Department of Applied Chemistry, Faculty of Science and Technology, Keio University, Yokohama, Japan

(Received November 4, 2010/Revised January 24, 2011/Accepted January 25, 2011/Accepted manuscript online February 2, 2011/Article first published online March 1, 2011)

Currently, patients with peritoneal dissemination of gastric cancer must accept a poor prognosis because there is no standard effective therapy. To inhibit peritoneal dissemination it is important to inhibit interactions between extracellular matrices (ECM) and cell surface integrins, which are important for cancer cell adhesion. Although nuclear factor-kappa B (NF-κB) is involved in various processes in cancer progression, its involvement in the expression of integrins has not been elucidated. We used a novel NF-κB inhibitor, dehydroxymethylepoxyquinomicin (DHMEQ), to study whether NF-κB blocks cancer cell adhesion via integrins in a gastric cancer dissemination model in mice and found that DHMEQ is a potent suppressor of cancer cell dissemination. Dehydroxymethylepoxyquinomicin suppressed the NF-κB activity of human gastric cancer cells NUGC-4 and 44As3Luc and blocked the adhesion of cancer cells to ECM when compared with the control. Dehydroxymethylepoxyquinomicin also inhibited expression of integrin (α2, α3, β1) in *in vitro* studies. In the *in vivo* model, we injected 44As3Luc cells pretreated with DHMEQ into the peritoneal cavity of mice and performed peritoneal lavage after the injection of cancer cells. Viable cancer cells in the peritoneal cavities were evaluated sequentially by *in vivo* imaging. In mice injected with DHMEQ-pretreated cells and lavaged, live cancer cells in the peritoneum were significantly reduced compared with the control, and these mice survived longer. These results indicate that DHMEQ could inhibit cancer cell adhesion to the peritoneum possibly by suppressing integrin expression. Nuclear factor-kappa B inhibition may be a new therapeutic option for suppressing postoperative cancer dissemination. (*Cancer Sci* 2011; 102: 1052–1058)

Peritoneal dissemination is the most frequent process through which gastric cancer recurs,[1] and patients with this condition must currently accept a very poor prognosis.[2,3] Standard chemotherapy is currently not sufficiently effective for improving the survival of patients with peritoneal dissemination of gastric cancer. To inhibit peritoneal dissemination, it may be important to control the adhesion of cancer cells to the peritoneum. During cancer cell dissemination in the abdominal cavity, cancer cells make contact with the basement membrane through gaps between mesothelial cells.[4,5] The basement membrane beneath mesothelial cells comprises extracellular matrices (ECM) consisting of type 1 and 4 collagen, fibronectin or laminin,[6] and mesothelial cells also produce ECM.[7] The interactions between these ECM and cell surface integrins play very important roles in cancer cell adhesion and, therefore, cancer progression.[8]

Integrins are membrane-bound proteins that form heterodimers of α- and β-subunits at the cell surface. The α-subunits vary between 120 and 180 kD, and are non-covalently associated with β-subunits (90–110 kD). To date, 14 α subunits and eight β subunits have been identified, and after mutual dimerization, these subunits contribute to cell adhesion or regulation of signal transduction required for cell survival by making contact with appropriate ECM.[9,10] It has been reported that integrins α2, α3 and β1 play important roles in the peritoneal dissemination of gastric cancer,[11] and that antibodies to these integrins suppress peritoneal dissemination of gastric cancer in a mouse model.[12]

Nuclear factor-kappaB (NF-κB) was first identified and reported in 1986[13] and studied in the context of immune and inflammatory responses.[14] Nuclear factor-kappaB is a generic term for dimers of NF-κB1 (p50/p105), NF-κB2 (p52/p100), c-Rel, RelA (p65/NF-κB3) and RelB.[15] To date, involvement of NF-κB in cancer-related molecules such as cyclin D1,[16] intercellular adhesion molecule-1 (ICAM-1), vascular cell adhesion molecule-1 (VCAM-1),[17] the Bcl family,[18] inhibitor of apoptosis (IAP), X-linked inhibitor of apoptosis protein (XIAP),[19] p53,[20] vascular endothelial growth factor (VEGF), interleukin (IL)-8,[21] MMP[22] and multidrug resistance protein 1 (MDR1),[23] has been elucidated. However, NF-κB has not been reported to be involved in cancer cell adhesion to the peritoneum via integrins.

A low-molecular-weight NF-κB inhibitor, dehydroxymethylepoxyquinomicin (DHMEQ), was newly developed by Umezawa.[24] Dehydroxymethylepoxyquinomicin specifically inhibits the nuclear translocation of p65 and prevents it binding to DNA[25]; it also has various anti-cancer effects in mouse models without obvious side-effects. Thus far, the following anti-cancer effects of DHMEQ have been reported: G1 arrest by inhibition of cyclin D1 expression;[26] and induction of apoptosis by inhibition of cIAP and XIAP,[27] or Bcl-2 and Bcl-xL.[28] Antitumor effects of DHMEQ have also been reported in *in vivo* models such as those for thyroid cancer,[27] prostate cancer,[29] hepatic cancer,[30] breast cancer,[31] pancreas cancer,[32] multiple myeloma,[28] malignant lymphoma[33] and leukemia.[26]

In the present study, we showed that NF-κB is associated with integrin expression in gastric cancer cell lines and that NF-κB inhibition by DHMEQ suppresses cancer progression by inhibiting the adhesion of gastric cancer cells to the peritoneum in a mouse model of peritoneal dissemination of gastric cancer.

[7]To whom correspondence should be addressed.
E-mail: ozaki-m@med.hokudai.ac.jp

doi: 10.1111/j.1349-7006.2011.01901.x

Materials and Methods

Cell cultures. The human gastric cancer cell line NUGC4 was obtained from the Japanese Cancer Research Resources Bank (JCRB, Osaka, Japan), and 44As3Luc with luciferase activity was constructed by one of the authors (K.Y.).[34] The 44As3Luc cells were derived from 44As3 cells, which is a highly peritoneal metastatic cell line, and were stably transfected with a pEGF-PLuc plasmid with CMV promoter (Clontech, Palo Alto, CA, USA). Human breast cancer cell lines MCF7 with constitutively low NF-κB activity and MDA-MB231 with constitutively high NF-κB activity were obtained from the American Type Culture Collection (Rockville, MD, USA).[31] The NUGC4 cells were cultured at 37°C in RPMI1640 (Sigma, St Louis, MO, USA) along with 10% fetal bovine serum (FBS); the 44As3Luc cells were cultured at the same temperature with RPMI1640 containing 100 μg/mL geneticin (Sigma); and the MCF7 and MDA-MB231 cells were also cultured at 37°C in 95% air and 5% CO_2 in DMEM (Sigma) along with 10% FBS.

Dehydroxymethylepoxyquinomycin (DHMEQ). We have originally designed and developed DHMEQ (molecular weight (MW): 261), a derivative of the natural antibiotic epoxyquinomycin C, to specifically target NF-κB.[24]

DNA-binding activity of NF-κB. To evaluate the DNA-binding activity of NF-κB in the steady state, 70% confluent cultures of NUGC4, 44As3Luc, MCF7 and MDA-MB231 in 10-cm dishes were stored at −80°C. To evaluate the effect of DHMEQ, the medium in the 70% confluent cultures of NUGC4 and 44As3Luc was replaced with 10 μg/mL DHMEQ solution, incubated for an appropriate time and stored at −80°C. The following day, nuclear proteins were extracted and examined using a p65 TransAM kit (ActiveMotif, Carlsbad, CA, USA). The absorbance was determined using a plate reader (Varioskan Flash, Thermo Fisher Scientific, Waltham, MA, USA). Each experiment was performed in triplicate.

NF-κB reporter gene assay. A GFP reporter gene construct was transfected using Cignal Reporter Assay kits (SA Biosciences, Frederick, MD, USA). Cultured cells were trypsinized and resuspended in Opti-MEM (Invitrogen, Carlsbad, CA, USA) with non-essential amino acids (Invitrogen) without antibiotics at a concentration of 2×10^5 cells in a 96-well plate. Cells were transfected with the reporter by culturing for 16 h with Surefect (SA Biosciences). After the medium was replaced with Opti-MEM with penicillin/streptomycin, the cells were incubated for an additional 8 h. The medium was then replaced with Opti-MEM containing 10 μg/mL of DHMEQ (or 0.024% of DMSO for the controls). The intensity of fluorescence was measured at appropriate times in triplicate using Varioskan Flash (excitation, 470 nm; emission, 515 nm).

mRNA expression of integrins in DHMEQ-treated cells. Real-time PCR was used to examine mRNA expression. The 44As3Luc cells were cultured in triplicate in 0.024% DMSO solution (controls) or in 10 μg/mL DHMEQ for the appropriate times. Total RNA was isolated using an RNeasy mini kit (Qiagen, Valencia, CA, USA) in accordance with the manufacturer's instructions. For cDNA synthesis, ReverTra Ace qPCR RT kit (Toyobo, Osaka, Japan) with Oligo(dT) 20 primer (Toyobo) was used in accordance with the manufacturer's instructions. For relative quantification by PCR, each cDNA product was analyzed in a LightCycler (version 1.4) using a QuantiTect SYBR Green PCR kit (Qiagen).

Flow cytometric analysis of integrin expression. p65 silencing was performed using p65 siRNA2 (BD Biosciences, Bedford, MA, USA). Next, 50% confluent cells were incubated for 24 h in medium without antibiotics in 10-cm dishes. Then, 33 nM p65 siRNA was added to each dish and transfected for 48 h. p65 silencing was confirmed by western blot analysis using primary antibodies against ×500 α-tubulin and ×1000 p65 protein (Cell Signaling, Beverly, MA, USA) and ×5000 goat anti-mouse IgG for tubulin or anti-rabbit IgG for the p65 protein. With regard to DHMEQ treatment, the medium in 70% confluent cell cultures in 10-cm dishes was replaced with 10 μg/mL DHMEQ solution (0.024% DMSO for the controls) and cultured for the appropriate times. These cells were trypsinized and analyzed using flow cytometry (FACS Caliber; Becton Dickinson, Franklin Lakes, NJ, USA). The antibodies used for these assays were integrin α2, integrin α3, integrin β1 and isotype controls for these integrins. All antibodies were obtained from R&D Systems (Minneapolis, MN, USA).

Adhesion assay. We evaluated the anti-adhesive effect of DHMEQ by using a plate pre-coated with ECM constituting the peritoneal basement membrane. The medium in 70% confluent cell cultures in 10-cm dishes was replaced with 10 μg/mL DHMEQ solution (or 0.024% DMSO for the controls), and the dishes were incubated for 24 h. These cells were trypsinized, assembled, adjusted to a concentration of 1×10^6 cells/mL with RPMI and distributed on the pre-coated plates (80 μL per plate). Next, the cells were incubated at 37°C for 1 h. Except for the non-treated plate, all plates were washed three times with 100 μL of FBS-free RPMI. After washing, 10 μL of ×50 diluted Cell Counting kit F (CCKF; Dojindo, Osaka, Japan) was added to each well, and the fluorescence intensity of the remaining live cells (adhesive cells) was evaluated using Varioskan Flash at 30 min after CCKF administration (excitation, 490 nm; emission, 515 nm). Pre-coated plates were manufactured by BD Biosciences and the ECM coated on the plates were types 1 and 4 collagen, fibronectin and laminin.

DHMEQ cytotoxicity assay. The cells were seeded into 96-well plates at 5×10^3 cells/well in 10% FBS-containing medium. Twenty-four hours later, the medium in the wells was replaced with different concentrations of DHMEQ solution or 0.048% DMSO solution, and the cells were then incubated again for 24 h. Lactate dehydrogenase (LDH) activity of the supernatant was measured using an LDH cytotoxicity detection kit (Takara Bio, Shiga, Japan).

Animal experiments. Six-week-old male BALB/c-nu/nu mice, each weighing approximately 20 g, were obtained from CLEA Japan, Inc. (Tokyo, Japan). The mice were grouped as follows: (i), implantation of DMSO-treated cells; (ii) implantation of DHMEQ-treated cells; (iii) implantation of DMSO-treated cells with peritoneal lavage; and (iv) implantation of DHMEQ-treated cells with peritoneal lavage. Each group comprised four mice. Then, 2×10^6 44As3Luc cells, which had been treated with 10 μg/mL DHMEQ (or 0.024% DMSO for the controls) for 24 h, were injected intraperitoneally into the above mentioned mice. One hour after injection, laparotomy and peritoneal lavage were performed using phosphate-buffered saline (PBS). Peritoneal lavage was performed through a 1-cm incision through which 5 mL of PBS was slowly injected. Bio-imaging was performed before and after the peritoneal lavage, and on days 2, 5, 10, 15 and 20 in order to evaluate cancer progression. Luminescence was evaluated at approximately 7 min after intraperitoneal injection of 1500 μg/mouse D-luciferin potassium salt (Synchem OHG, Altenburg, Germany). *In vivo* imaging was performed using Photon Imager Hu (Biospace Lab, Paris, France) with the mice under isoflurane anesthesia (Abbott Japan, Tokyo, Japan). Images were captured using Photo Acquisition 2.6 (Biospace Lab) with 0.5 min exposure and processed using Photo Vision Plus. Signal intensity was quantified as the sum of all detected photon counts (count per minute [CPM]) within the region of interest (ROI). All procedures involving animals and their care were approved by the Ethics Committee of Hokkaido University in accordance with institutional and Japanese governmental guidelines for animal experiments.

Scanning electron microscopy (SEM) of the peritoneal wall. The peritoneal walls of mice injected with cancer cells

were fixed with 10% formaldehyde for 180 min and then overnight at 4°C with 1.25% glutaraldehyde solution. The fixed samples were dehydrated in a 30–100% graded ethanol series and immersed in tert-butyl alcohol overnight at −20°C. These samples were dried using ES-2000 (Hitachi High-Technologies Co., Tokyo, Japan) for 3 h and ion-sputtered using E-1030 (Hitachi) for 120 s. The peritoneal surface was observed under a scanning electron microscope (S-3500N; Hitachi).

Statistics. The mean and SD were calculated for all variables, except the data from the flow cytometry. Between-group statistical significance was determined using the Student's *t* test. $P < 0.05$ was considered as statistically significant.

Results

DHMEQ effectively suppresses p65-DNA binding activity in gastric cancer cells. In the steady state, the p65-DNA binding activities in NUGC4 and 44As3Luc cells were as high as that in MDA-MB231 cells, a positive control cell with high binding activity. The activity in MCF7 cells is constitutively low as previously reported [31], and hence these cells were used as the negative control (Fig. 1A). The binding activities in both cells reached their lowest levels 2 h after the addition of 10 μg/mL DHMEQ (as a final concentration) and returned to initial conditions within 24 h (Fig. 1B). A GFP reporter assay showed that DHMEQ significantly suppresses transcriptional activity in both cells (Fig. 1C). On the basis of these results, we considered that DHMEQ had a similar effect in NUGC4 and 44As3Luc cells. Therefore, we used 44As3Luc cells in the following experiments. We planned to evaluate cancer progression using bioimaging.

Effect of NF-κB inhibition on integrin expression. In 44As3Luc cells, the mRNA of all integrins – α2, α3 and β1 – were significantly suppressed 2 h after the addition of 10 μg/mL DHMEQ (as a final concentration) compared with the control to which DMSO was added (Fig. 2A). The percentage reduction in the expressions of integrins α2, α3 and β1 was 27%, 31% and 8%, respectively. Flow cytometric analysis revealed that the expressions of all cell surface integrins on 44As3Luc cells were gradually suppressed after the addition of DHMEQ (Fig. 2B). Reductions in integrin expression (α2, α3 and β1) following DHMEQ addition was 68%, 83% and 45% at 24 h, respectively. Similarly, flow cytometric analysis of integrins α2, α3 and β1 revealed that the expressions of cell surface integrins in p65-deleted cells were suppressed to the same degree as in DHMEQ-treated cells (Fig. 2C). Reductions in integrin expression after p65 deletion were 34% (α2), 76% (α3) and 41% (β1). p65 silencing was confirmed by western blotting for nuclear and cytoplasmic p65 proteins (Fig. 2D).

Anti-adhesive effect of DHMEQ-treated cells in an *in vitro* assay. Significantly fewer 44As3Luc cells treated with 10 μg/mL DHMEQ (final concentration) remained alive on plates pre-coated with ECM after they were washed (ECM-adhesive cells) than 44As3Luc cells treated with DMSO (Fig. 3A). Reductions in the numbers of adhesive cells following DHMEQ addition were 18.3% (laminin), 34.8% (fibronectin), 38.2% (type 1 collagen) and 43.5% (type 4 collagen). The LDH value, which represents the cytotoxic effect, was significantly elevated in the supernatant of cells treated with DHMEQ at concentrations >17.5 μg/mL (Fig. 3B).

Effect of peritoneal lavage on implantation of DHMEQ-treated cancer cells on the abdominal wall. The number of cancer cells decreased in mice injected with DHMEQ-pretreated cells and subjected to peritoneal lavage (Fig. 4A). The intensity of bioluminescence after lavage was significantly reduced (reduction rate, 39%) in mice that were injected with DHMEQ-pretreated cells and subjected to peritoneal lavage compared with in mice injected with DMSO-pretreated control cells and subjected to

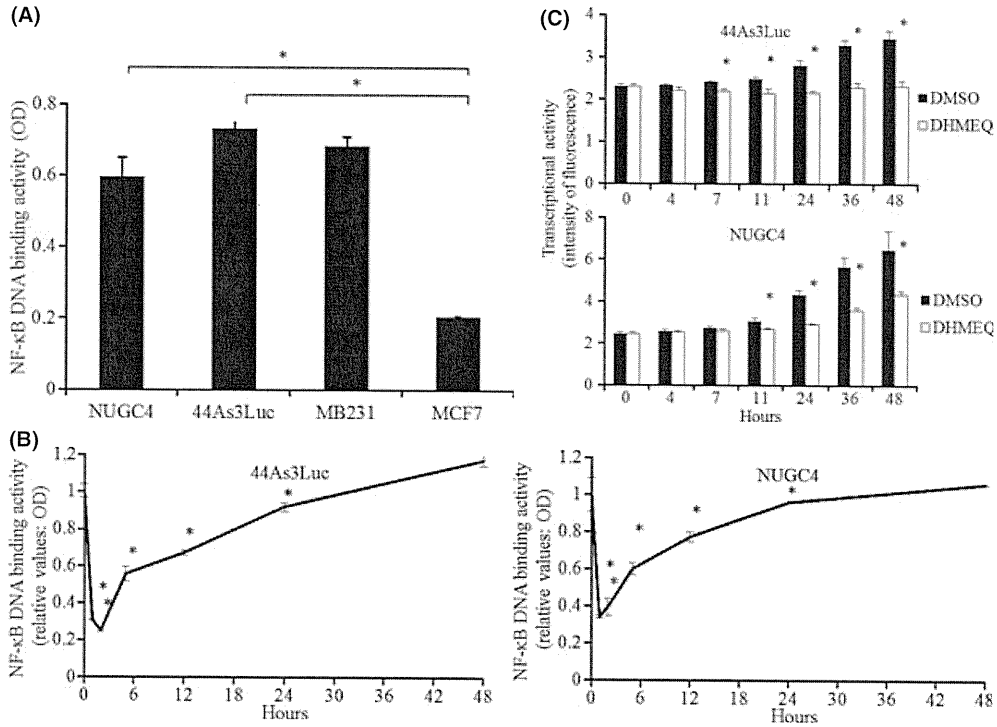

Fig. 1. Dehydroxymethylepoxyquinomicin (DHMEQ) effectively suppressed p65-DNA binding activity in gastric cancer cells. (A) Nuclear p65 protein binding activity to DNA in a steady state. MDA-MB231 cells were used as a positive control, and MCF7 cells were used as a negative one. *$P < 0.05$. (B) Time course of binding activity of nuclear p65 proteins to DNA in DHMEQ-treated cells. The binding activities of both cells were assessed at 2, 6, 12, 24 and 48 h after DHMEQ administration. *Significantly <0 h ($P < 0.05$). (C) Nuclear factor-kappa B (NF-κB) GFP reporter assay. The black bars show cells treated with DMSO, and white bars show those with DHMEQ. *Significantly more than controls ($P < 0.05$). OD, optical density.

doi: 10.1111/j.1349-7006.2011.01901.x

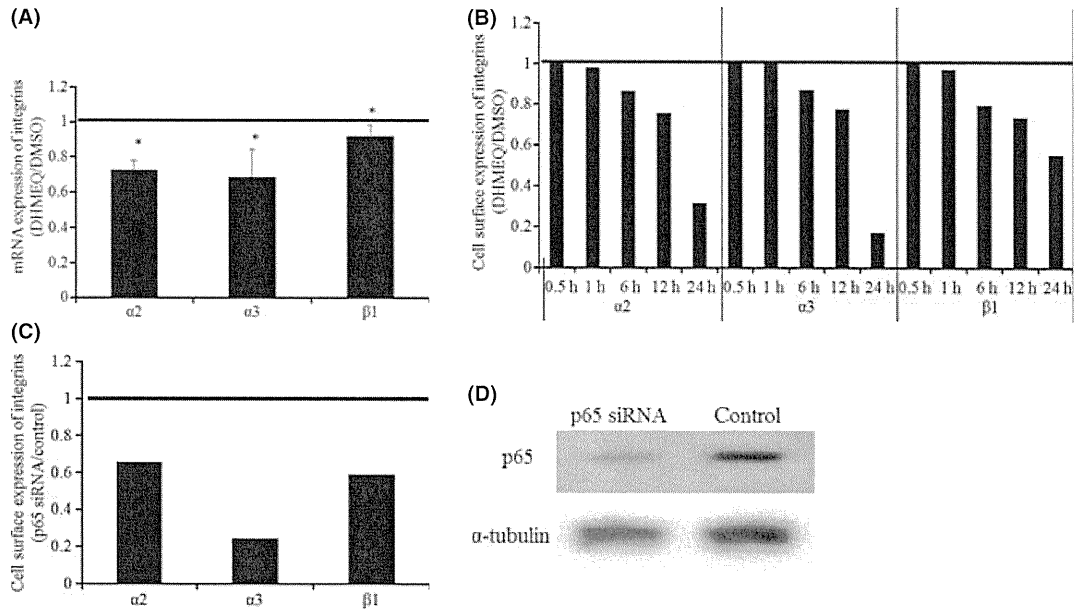

Fig. 2. Effect of nuclear factor-kappa B (NF-κB) inhibition on expression of adhesion molecules. (A) Quantitative evaluation of mRNA of integrins by real-time PCR. The graph shows the average of the ratio of copies of dehydroxymethylepoxyquinomicin (DHMEQ)-treated 44As3Luc cells to DMSO-treated cells at 2 h after DHMEQ administration. When the longitudinal value is below 1 (bold line), the integrin expression of DHMEQ-treated cells is lower than that of DMSO-treated cells. *Significantly less than controls ($P < 0.05$). (B) Expression of cell surface integrins of DHMEQ-treated cells. The graph shows the expression rate of cell surface adhesion molecules of 44As3Luc cells treated with DHMEQ compared with that of DMSO-treated cells for each time point. The bold line is as described above. (C) Expression of cell surface adhesion molecules of cells knocked down by p65 siRNA. The graph shows the rate of cell surface integrins of 44As3Luc cells knocked down by p65 siRNA. The bold line is as described above. (D) p65 deletion. The p65 deletion was confirmed by western blotting.

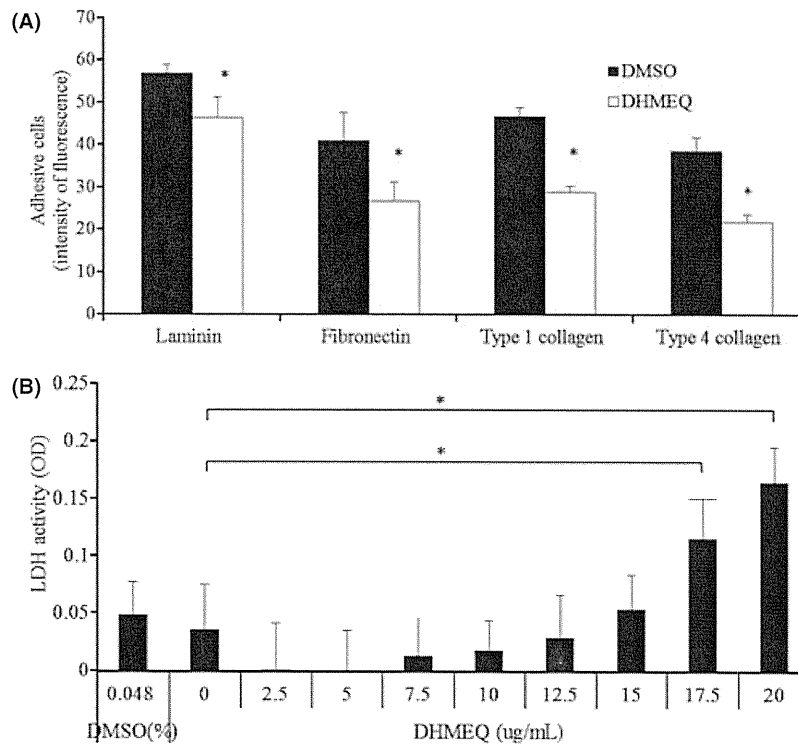

Fig. 3. Anti-adhesive effect of dehydroxymethyl-epoxyquinomicin (DHMEQ) pretreated cells in the *in vitro* study. (A) Adhesion assay. The bars show the fluorescence intensity of the remaining live cells on the plates. The black bars show cells pretreated with DHMEQ, and white bars show those with DMSO. *Significantly less than controls ($P < 0.05$). (B) Evaluation of cytotoxicity of DHMEQ. The graph shows lactate dehydrogenase (LDH) activity of the supernatant of the 44As3Luc cells treated with DHMEQ or DMSO. *$P < 0.05$. OD, optical density.

peritoneal lavage (Fig. 4B). The SEM revealed that cancer cells adhered less to the basement membrane of the peritoneum in mice injected with DHMEQ-pretreated cells than in those injected with DMSO-pretreated control cells (Fig. 4C).

Follow up of gastric cancer dissemination by *in vivo* imaging. The DHMEQ-pretreated 44As3Luc cells injected in mice grew slowly compared with the DMSO-pretreated cells (Fig. 5A). The increase in the CPM/mm^2 value of the

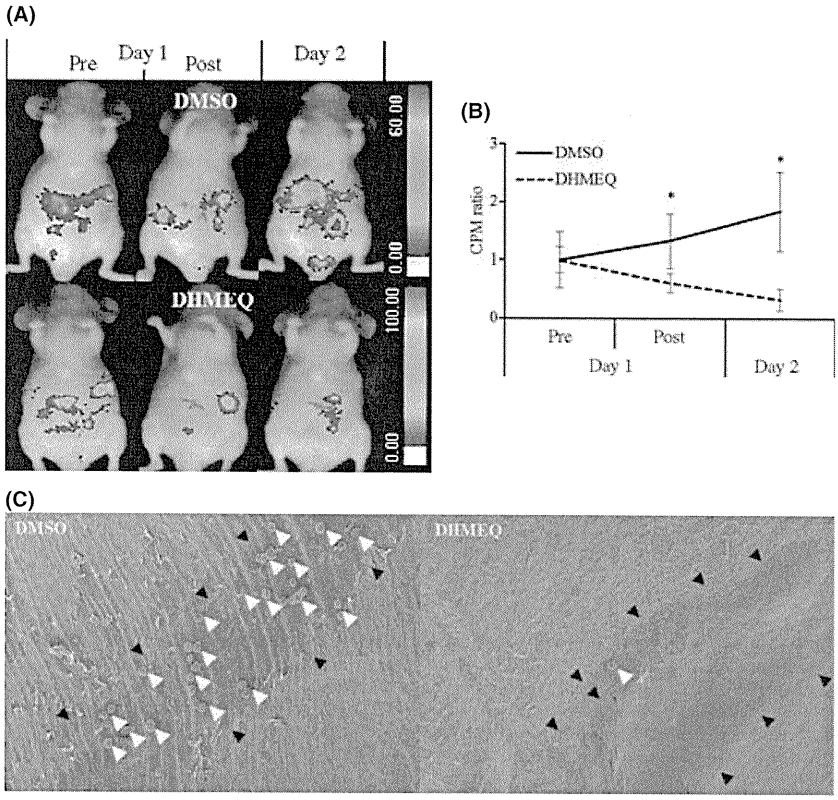

Fig. 4. Peritoneal lavage inhibited cancer cells pretreated with dehydroxymethylepoxyquinomicin (DHMEQ) from implanting into the abdominal wall. (A) *In vivo* imaging at around the time of peritoneal lavage. The luminescent value indicates the number of live cells in the abdominal wall. Pre/Post means before/after the peritoneal lavage. (B) Count per minute (CPM)/mm^2 value of pre/post peritoneal lavage. The graph shows the time course of the CPM/mm^2 value compared with the time of cancer cell injection. Initial values were adjusted to 1. *Significantly less than controls ($P < 0.05$). (C) SEM findings of the peritoneum. Left: abdominal wall injected with 44As3Luc cells pretreated with DHMEQ. Right: those with DMSO. The area indicated by black arrowheads is the area exposed to the peritoneal cavity. White arrowheads show the adhesive cancer cells.

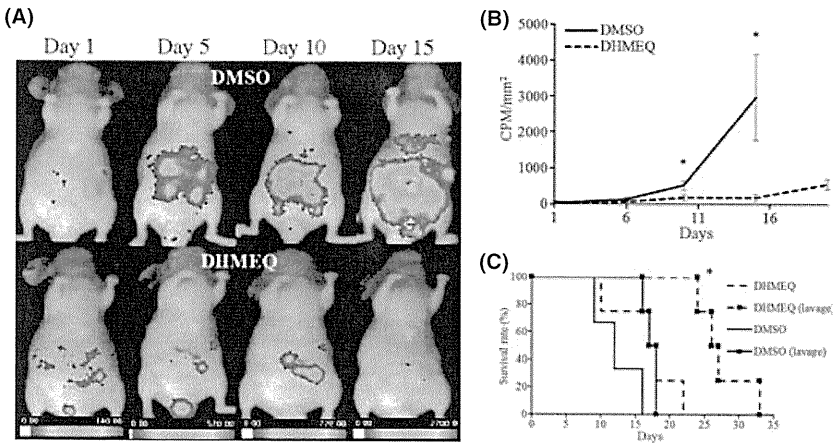

Fig. 5. Follow up after peritoneal lavage. (A) Follow-up imaging of mice subjected to peritoneal lavage. The range bars were adjusted for mice injected with DMSO pretreated cells at every evaluation day. (B) Time course of the count per minute (CPM)/mm^2 value. The black line represents the mice that were injected with DMSO-pretreated cells, and the broken line represents those injected with dehydroxymethylepoxyquinomicin (DHMEQ)-pretreated cells. *Significantly less than controls ($P < 0.05$). (C) Kaplan–Meier analysis of the survival of all groups. The line is as described above. The line with markers represents mice subjected to peritoneal lavage. *Significantly prolonged than all other groups ($P < 0.05$).

DHMEQ-treated cells was significantly delayed. The error bar of the CPM/mm^2 value of the DMSO-pretreated group ranged widely, because malignant ascites possibly obscured luminescent emission at the terminal stage (Fig. 5B). Survival was only significantly prolonged in mice injected with DHMEQ-treated cells and subjected to peritoneal lavage (Fig. 5C).

Discussion

NF-κB is undoubtedly involved in various biological properties of cancer cells.[35] However, its involvement in the expression of integrins, which are associated with cancer cell adhesion to the peritoneum, has not been reported. In the present study, we investigated whether NF-κB is involved in cell adhesion to the peritoneum via regulation of integrin expression, and whether DHMEQ, as a novel NF-κB inhibitor, suppresses the dissemination of gastric cancer in a mouse model.

Several investigators reported that NF-κB activity is associated with peritoneal dissemination of cancer cells.[36–38] Sasaki *et al.*[39] evaluated human gastric cancer tissues by immunohistochemical analysis, where NF-κB activation was significantly correlated with peritoneal metastases and survival. Our results in the present study support the previously reported data that NF-κB activity of gastric cancer cell lines was markedly activated and with highly metastatic behavior, and that DHMEQ sufficiently inhibited NF-κB activity and eventually suppressed the peritoneal dissemination.

Integrins are also associated with malignant potential.[40–42] Integrins play an important role in cancer cell adhesion to the peritoneum by enabling contact with appropriate ECM. Oosterling *et al.*[43] showed that anti-β1 integrin antibody reduces surgery-induced adhesion of colon carcinoma cells to traumatized peritoneal surfaces. Fishman *et al.*[44] showed similar findings using ovarian cancer cell lines in the *in vitro* analysis. With

doi: 10.1111/j.1349-7006.2011.01901.x

regard to gastric cancer, integrins α2, α3 and β1 are key molecules in animal models and humans.[11,12,45,46] The ligands of integrin α2β1 are collagens and laminin, and those of α3β1 are fibronectin, laminin,and collagens.[10] In our *in vitro* study, DHMEQ suppressed cancer cell adhesion to the peritoneum via p65-mediated suppression of integrin expression. Also, Takatsuki *et al.*[12] reported that anti-α3 antibody strongly suppressed the adhesion of gastric cancer cells to mice peritoneum. This integrin α3 was suppressed most by DHMEQ in this study. Therefore, DHMEQ may suppress cancer cell adhesion mainly via integrin α3, while DHMEQ may associate with other adhesion molecules that are not examined in this study.

In our *in vivo* study, viable cells in mice injected with DHMEQ-treated cells and subjected to peritoneal lavage still decreased on day 2 and only this group survived significantly longer. This finding might suggest that DHMEQ exerts another effect via the anti-adhesive effect. Jiang *et al.*[47] reported that NF-κB inhibition by IκBβ reduces anchorage-independent growth in a lung cancer cell line. Scaife *et al.*[48] showed that NF-κB inhibitor causes anoikis in a human colon cancer cell line. It might be possible that DHMEQ is associated with a pro-anoikis effect in gastric cancer dissemination.

In the present study, we first demonstrated that NF-κB could play a pivotal role in the progression of gastric cancer via the regulation of integrin expression and promotion of adhesion of cancer cells to the peritoneal wall. In our *in vivo* study, a specific deletion of NF-κB (p65) by siRNA was not performed, because we considered that transient deletion of p65 protein does not reflect the same result of DHMEQ-administered cells. Additionally, we could not clarify whether the DHMEQ effect on integrins is unique to the integrin pathway or concomitant with other phenomenon such as apoptosis. Further studies are required to clarify the involvement of integrins or other molecules in the anti-adhesive effect of DHMEQ against cancer cells. We believe that NF-κB inhibitors such as DHMEQ may be potential therapeutic options to prevent gastric cancer progression during peri-operative periods.

Acknowledgments

This study were supported by the Program for Promotion of Fundamental Studies in Health Sciences of the National Institute of Biomedical Innovation (NIBIO) and by a Grant-in-Aid for Scientific Research from the Ministry of Education, Culture, Sports, Science and Technology of Japan (#17390357 and #19659317 to M.O., # 21390369 to T.K.). We also thank Dr M. Takigahira (Section for Studies on Metastasis, National Cancer Center Research Institute, Chuo-ku, Tokyo, Japan) for her excellent technical support for constructing the 44As3Luc cells, Ms N. Kobayashi (Department of General Surgery, Graduate School of Medicine, Hokkaido University, Sapporo, Japan) for performing the real-time PCR assay and Dr H. Maeda (Creative Research Institution, Hokkaido University, Sapporo, Japan) for processing the samples for SEM.

Disclosure Statement

The authors have no conflict of interest.

References

1 Sasako M. Principles of surgical treatment for curable gastric cancer. *J Clin Oncol* 2003; **21**: 274s–5s.
2 Schott A, Vogel I, Krueger U *et al.* Isolated tumor cells are frequently detectable in the peritoneal cavity of gastric and colorectal cancer patients and serve as a new prognostic marker. *Ann Surg* 1998; **227**: 372–9.
3 Sadeghi B, Arvieux C, Glehen O *et al.* Peritoneal carcinomatosis from non-gynecologic malignancies: results of the EVOCAPE 1 multicentric prospective study. *Cancer* 2000; **88**: 358–63.
4 Kimura A, Koga S, Kudoh H, Iitsuka Y. Peritoneal mesothelial cell injury factors in rat cancerous ascites. *Cancer Res* 1985; **45**: 4330–3.
5 Yonemura Y, Endo Y, Obata T, Sasaki T. Recent advances in the treatment of peritoneal dissemination of gastrointestinal cancers by nucleoside antimetabolites. *Cancer Sci* 2007; **98**: 11–8.
6 Witz CA, Montoya-Rodriguez IA, Cho S, Centonze VE, Bonewald LF, Schenken RS. Composition of the extracellular matrix of the peritoneum. *J Soc Gynecol Investig* 2001; **8**: 299–304.
7 Lessan K, Aguiar DJ, Oegema T, Siebenson L, Skubitz AP. CD44 and beta1 integrin mediate ovarian carcinoma cell adhesion to peritoneal mesothelial cells. *Am J Pathol* 1999; **154**: 1525–37.
8 Ruoslahti E, Giancotti FG. Integrins and tumor cell dissemination. *Cancer Cells* 1989; **1**: 119–26.
9 Hehlgans S, Haase M, Cordes N. Signalling via integrins: implications for cell survival and anticancer strategies. *Biochim Biophys Acta* 2007; **1775**: 163–80.
10 Hynes RO. Integrins: versatility, modulation, and signaling in cell adhesion. *Cell* 1992; **69**: 11–25.
11 Nishimura S, Chung YS, Yashiro M, Inoue T, Sowa M. Role of alpha 2 beta 1- and alpha 3 beta 1-integrin in the peritoneal implantation of scirrhous gastric carcinoma. *Br J Cancer* 1996; **74**: 1406–12.
12 Takatsuki H, Komatsu S, Sano R, Takada Y, Tsuji T. Adhesion of gastric carcinoma cells to peritoneum mediated by alpha3beta1 integrin (VLA-3). *Cancer Res* 2004; **64**: 6065–70.
13 Sen R, Baltimore D. Multiple nuclear factors interact with the immunoglobulin enhancer sequences. *Cell* 1986; **46**: 705–16.
14 Berkholtz CB, Lai BE, Woodruff TK, Shea LD. Distribution of extracellular matrix proteins type I collagen, type IV collagen, fibronectin, and laminin in mouse folliculogenesis. *Histochem Cell Biol* 2006; **126**: 583–92.
15 Verma IM, Stevenson JK, Schwarz EM, Van Antwerp D, Miyamoto S. Rel/NF-kappa B/I kappa B family: intimate tales of association and dissociation. *Genes Dev* 1995; **9**: 2723–35.
16 Donnellan R, Chetty R. Cyclin D1 and human neoplasia. *Mol Pathol* 1998; **51**: 1–7.
17 Bonizzi G, Karin M. The two NF-kappaB activation pathways and their role in innate and adaptive immunity. *Trends Immunol* 2004; **25**: 280–8.
18 Karin M, Cao Y, Greten FR, Li ZW. NF-kappaB in cancer: from innocent bystander to major culprit. *Nat Rev Cancer* 2002; **2**: 301–10.
19 Deveraux QL, Reed JC. IAP family proteins – suppressors of apoptosis. *Genes Dev* 1999; **13**: 239–52.
20 Tergaonkar V, Pando M, Vafa O, Wahl G, Verma I. p53 stabilization is decreased upon NFkappaB activation: a role for NFkappaB in acquisition of resistance to chemotherapy. *Cancer Cell* 2002; **1**: 493–503.
21 Huang S, Robinson JB, Deguzman A, Bucana CD, Fidler IJ. Blockade of nuclear factor-kappaB signaling inhibits angiogenesis and tumorigenicity of human ovarian cancer cells by suppressing expression of vascular endothelial growth factor and interleukin 8. *Cancer Res* 2000; **60**: 5334–9.
22 Rangaswami H, Bulbule A, Kundu GC. Nuclear factor-inducing kinase plays a crucial role in osteopontin-induced MAPK/IkappaBalpha kinase-dependent nuclear factor kappaB-mediated promatrix metalloproteinase-9 activation. *J Biol Chem* 2004; **279**: 38921–35.
23 Bentires-Alj M, Barbu V, Fillet M *et al.* NF-kappaB transcription factor induces drug resistance through MDR1 expression in cancer cells. *Oncogene* 2003; **22**: 90–7.
24 Ariga A, Namekawa J, Matsumoto N, Inoue J, Umezawa K. Inhibition of tumor necrosis factor-alpha-induced nuclear translocation and activation of NF-kappa B by dehydroxymethylepoxyquinomicin. *J Biol Chem* 2002; **277**: 24625–30.
25 Yamamoto M, Horie R, Takeiri M, Kozawa I, Umezawa K. Inactivation of NF-kappaB Components by Covalent Binding of (−)-Dehydroxymethylepoxyquinomicin to Specific Cysteine Residues. *J Med Chem* 2008; **51**: 5780–8.
26 Watanabe M, Ohsugi T, Shoda M *et al.* Dual targeting of transformed and untransformed HTLV-1-infected T cells by DHMEQ, a potent and selective inhibitor of NF-kappaB, as a strategy for chemoprevention and therapy of adult T-cell leukemia. *Blood* 2005; **106**: 2462–71.
27 Starenki DV, Namba H, Saenko VA *et al.* Induction of thyroid cancer cell apoptosis by a novel nuclear factor kappaB inhibitor, dehydroxymethylepoxyquinomicin. *Clin Cancer Res* 2004; **10**: 6821–9.
28 Tatetsu H, Okuno Y, Nakamura M *et al.* Dehydroxymethylepoxyquinomicin, a novel nuclear factor-kappaB inhibitor, induces apoptosis in multiple myeloma cells in an IkappaBalpha-independent manner. *Mol Cancer Ther* 2005; **4**: 1114–20.
29 Kikuchi E, Horiguchi Y, Nakashima J *et al.* Suppression of hormone-refractory prostate cancer by a novel nuclear factor kappaB inhibitor in nude mice. *Cancer Res* 2003; **63**: 107–10.
30 Nishimura D, Ishikawa H, Matsumoto K *et al.* DHMEQ, a novel NF-kappaB inhibitor, induces apoptosis and cell-cycle arrest in human hepatoma cells. *Int J Oncol* 2006; **29**: 713–9.

31 Matsumoto G, Namekawa J, Muta M *et al.* Targeting of nuclear factor kappaB Pathways by dehydroxymethylepoxyquinomicin, a novel inhibitor of breast carcinomas: antitumor and antiangiogenic potential in vivo. *Clin Cancer Res* 2005; **11**: 1287–93.
32 Matsumoto G, Muta M, Umezawa K *et al.* Enhancement of the caspase-independent apoptotic sensitivity of pancreatic cancer cells by DHMEQ, an NF-kappaB inhibitor. *Int J Oncol* 2005; **27**: 1247–55.
33 Dabaghmanesh N, Matsubara A, Miyake A *et al.* Transient inhibition of NF-kappaB by DHMEQ induces cell death of primary effusion lymphoma without HHV-8 reactivation. *Cancer Sci* 2009; **100**: 737–46.
34 Yanagihara K, Takigahira M, Takeshita F *et al.* A photon counting technique for quantitatively evaluating progression of peritoneal tumor dissemination. *Cancer Res* 2006; **66**: 7532–9.
35 Nakanishi C, Toi M. Nuclear factor-kappaB inhibitors as sensitizers to anticancer drugs. *Nat Rev Cancer* 2005; **5**: 297–309.
36 Mabuchi S, Ohmichi M, Nishio Y *et al.* Inhibition of inhibitor of nuclear factor-kappaB phosphorylation increases the efficacy of paclitaxel in in vitro and in vivo ovarian cancer models. *Clin Cancer Res* 2004; **10**: 7645–54.
37 Nakahara C, Nakamura K, Yamanaka N *et al.* Cyclosporin-A enhances docetaxel-induced apoptosis through inhibition of nuclear factor-kappaB activation in human gastric carcinoma cells. *Clin Cancer Res* 2003; **9**: 5409–16.
38 Shao M, Cao L, Shen C *et al.* Epithelial-to-mesenchymal transition and ovarian tumor progression induced by tissue transglutaminase. *Cancer Res* 2009; **69**: 9192–201.
39 Sasaki N, Morisaki T, Hashizume K *et al.* Nuclear factor-kappaB p65 (RelA) transcription factor is constitutively activated in human gastric carcinoma tissue. *Clin Cancer Res* 2001; **7**: 4136–42.
40 Pontes-Junior J, Reis ST, de Oliveira LC *et al.* Association between integrin expression and prognosis in localized prostate cancer. *Prostate* 2010; **70**: 1189–95.
41 Dingemans AM, van den Boogaart V, Vosse BA, van Suylen RJ, Griffioen AW, Thijssen VL. Integrin expression profiling identifies integrin alpha5 and beta1 as prognostic factors in early stage non-small cell lung cancer. *Mol Cancer* 2010; **9**: 152.
42 Takayama N, Arima S, Haraoka S, Kotho T, Futami K, Iwashita A. Relationship between the expression of adhesion molecules in primary esophageal squamous cell carcinoma and metastatic lymph nodes. *Anticancer Res* 2003; **23**: 4435–42.
43 Oosterling SJ, van der Bij GJ, Bogels M *et al.* Anti-beta1 integrin antibody reduces surgery-induced adhesion of colon carcinoma cells to traumatized peritoneal surfaces. *Ann Surg* 2008; **247**: 85–94.
44 Fishman DA, Kearns A, Chilukuri K *et al.* Metastatic dissemination of human ovarian epithelial carcinoma is promoted by alpha2beta1-integrin-mediated interaction with type I collagen. *Invasion Metastasis* 1998; **18**: 15–26.
45 Kawamura T, Endo Y, Yonemura Y *et al.* Significance of integrin alpha2/beta1 in peritoneal dissemination of a human gastric cancer xenograft model. *Int J Oncol* 2001; **18**: 809–15.
46 Matsuoka T, Yashiro M, Nishimura S *et al.* Increased expression of alpha2beta1-integrin in the peritoneal dissemination of human gastric carcinoma. *Int J Mol Med* 2000; **5**: 21–5.
47 Jiang Y, Cui L, Yie TA, Rom WN, Cheng H, Tchou-Wong KM. Inhibition of anchorage-independent growth and lung metastasis of A549 lung carcinoma cells by IkappaBbeta. *Oncogene* 2001; **20**: 2254–63.
48 Scaife CL, Kuang J, Wills JC *et al.* Nuclear factor kappaB inhibitors induce adhesion-dependent colon cancer apoptosis: implications for metastasis. *Cancer Res* 2002; **62**: 6870–8.

doi: 10.1111/j.1349-7006.2011.01901.x

Molecular Vision 2012; 18:455-464 <http://www.molvis.org/molvis/v18/a49>
Received 8 January 2012 | Accepted 10 February 2012 | Published 14 February 2012

Amelioration of ultraviolet-induced photokeratitis in mice treated with astaxanthin eye drops

Anton Lennikov,[1] Nobuyoshi Kitaichi,[1,2,3] Risa Fukase,[1] Miyuki Murata,[1,2] Kousuke Noda,[1] Ryo Ando,[1] Takeshi Ohguchi,[1] Tetsuya Kawakita,[4] Shigeaki Ohno,[2] Susumu Ishida[1]

[1]Laboratory of Ocular Cell Biology and Visual Science, Department of Ophthalmology, Hokkaido University Graduate School of Medicine, Sapporo, Japan; [2]Department of Ocular Inflammation and Immunology, Hokkaido University Graduate School of Medicine, Sapporo, Japan; [3]Department of Ophthalmology, Health Sciences University of Hokkaido, Sapporo, Japan; [4]Department of Ophthalmology, Keio University, School of Medicine, Tokyo, Japan

Purpose: Ultraviolet (UV) acts as low-dose ionizing radiation. Acute UVB exposure causes photokeratitis and induces apoptosis in corneal cells. Astaxanthin (AST) is a carotenoid, present in seafood, that has potential clinical applications due to its high antioxidant activity. In the present study, we examined whether topical administration of AST has preventive and therapeutic effects on UV-photokeratitis in mice.

Methods: C57BL/6 mice were administered with AST diluted in polyethylene glycol (PEG) in instillation form (15 µl) to the right eye. Left eyes were given vehicle alone as controls. Immediately after the instillation, the mice, under anesthesia, were irradiated with UVB at a dose of 400 mJ/cm^2. Eyeballs were collected 24 h after irradiation and stained with H&E and TUNEL. In an in vitro study, mouse corneal epithelial (TKE2) cells were cultured with AST before UV exposure to quantify the UV-derived cytotoxicity.

Results: UVB exposure induced cell death and thinning of the corneal epithelium. However, the epithelium was morphologically well preserved after irradiation in AST-treated corneas. Irradiated corneal epithelium was significantly thicker in eyes treated with AST eye drops, compared to those treated with vehicles ($p<0.01$), in a doses dependent manner. Significantly fewer apoptotic cells were observed in AST-treated eyes than controls after irradiation ($p<0.01$). AST also reduced oxidative stress in irradiated corneas. The in vitro study showed less cytotoxicity of TKE2 cells in AST-treated cultures after UVB-irradiation ($p<0.01$). The cytoprotective effect increased with the dose of AST.

Conclusions: Topical AST administration may be a candidate treatment to limit the damages by UV irradiation with wide clinical applications.

Ultraviolet (UV) irradiation represents a significant environmental hazard that can cause acute and chronic inflammatory changes in the cornea, lens, and retina of the eye. The sources of UV radiation are not merely from electric welding and tanning lamps but also from sunny days on the sea or in snowy mountains when eyes are left unprotected. In recent decades, the risk of acute photochemically-induced ocular damage has increased due to stratospheric ozone depletion [1]. UVB exposure causes photokeratitis, which is associated with expression of nuclear factor (NF)-κB, prostaglandin E2 (PGE2), and many other inflammatory agents [1]. Acute UVB exposure causes damage deeper than the epithelium, involving all tissues of the cornea [2] and inducing apoptosis in corneal cells [3,4]. Although the energy is much less than that of the gamma rays, ophthalmologists find it is necessary to study ways to prevent the damages caused by UV radiation due to its association with clinical ocular diseases. We have already reported that applying UVB irradiation at 400 mJ/cm^2 to mice corneas can be a useful model for studying corneal inflammation [3].

Antioxidant enzymes, such as superoxide dismutase [5] and catalase [6], and pharmacologic antioxidants like N-acetyl cysteine [7,8], inhibit tumor necrosis factor (TNF)-α activation through NF-κB-dependent gene expression [9]. Astaxanthin (AST), 3,30-dihydroxy-b,b-carotene-4,40-dione, a carotenoid without vitamin A activity [10,11], has potential clinical applications due to its antioxidant activity, which is higher than β-carotene and α-tocopherol [10,12,13]. In addition, it has many highly potent pharmacological effects, including anti-tumor, anti-cancer, anti-diabetic, and anti-inflammation activities [12,14-16]. The potent activity of AST has been observed to modulate biologic functions ranging from lipid peroxidation to tissue protection [14,17]. The presence of the hydroxyl (OH) and keto (C=O) on each ionone ring in AST explains its unique feature of antioxidant activity for the protection of both the inner and outer membrane surfaces [10,14,18,19]. AST is found abundantly in the red-orange pigment of marine animals such as salmon (and salmon roe) and the shell of crabs and shrimp. AST and AST-like products are commonly indicated as

Correspondence to: Nobuyoshi Kitaichi, M.D., Ph.D., Department of Ocular Inflammation and Immunology, Hokkaido University Graduate School of Medicine, Kita-15, Nishi-7, Kita-ku, Sapporo 060-8638, Japan; Phone: +81-11-706-5944; FAX: +81-11-706-5948; email: nobukita@med.hokudai.ac.jp

antioxidants [20] and immune modulators [21]. One of the effects of AST is to scavenge reactive oxygen species [22]. We previously reported that AST showed a dose-dependent anti-inflammatory effect [23,24]. It was also reported that AST inhibited the production of inflammatory mediators by blocking NF-κB activation in vitro [4]. In the present study, we examined whether topical administration of AST has therapeutic effects on UV photokeratitis in mice.

METHODS

Animals and reagents: Six- to 8-week-old C57BL/6 male mice were obtained from Clear Japan (Tokyo, Japan). Mice were maintained under specific pathogen-free conditions. All procedures involving animals were performed in accordance with the ARVO resolution on the use of animals in research. AST was purchased from Sigma-Aldrich (Tokyo, Japan).

UV irradiation: The mice were administered with AST diluted in polyethylene glycol (PEG) in instillation form (15 µl) to the right eye once at the following concentrations: 1, 0.1, and 0.01 mg/ml (10 mice per group. Left eyes were instilled with vehicle alone. Immediately after the instillation, anesthetized mice were irradiated with UVB at a dose of 400 mJ/cm^2 from a FS-20 (Panasonic, Osaka, Japan) fluorescent lamp. These bulbs have a broad emission spectrum (250–400 nm) with high output primarily in the UVB spectrum (290–320 nm). To evaluate the effects of AST on the corneal surface without UVB damage, control mice received the instillation of 1 mg/ml of AST without irradiation. All experiments were performed in triplicate.

H&E and TUNEL staining: The eyes were dissected from mice 24 h after UVB exposure and fixed with 4% paraformalin. Tissue sections were prepared and stained with hematoxylin-eosin (H&E) for morphological analysis. Other sections were stained by terminal deoxynucleotidyl transferase dUTP nick end labeling (TUNEL) assay to detect apoptotic signaling. Apoptotic cells were detected with a Cell Death Detection Kit (Roche Diagnostics Japan, Tokyo) containing all necessary reagents for staining. Slides imaging, cell counting, and thickness evaluations were performed with BZ-9000 fluorescence microscope (Keyence, Japan) and software bundled with the apparatus. At least 10 sections were used to evaluate the epithelial thickness, measurements of 10 randomly selected areas of epithelium of central cornea was performed and averaged.

Evaluation of the "sunglasses effect" of AST: The "sunglass effect" represents the status when protective properties of a substance are only due to blocking the UV rather than having a cytoprotective effect. To evaluate this effect, and whether AST is capable of rescuing the damaged epithelia after UVB irradiation, we performed additional experiments where mice were first irradiated with UVB at a dose of 400 mJ/cm^2 under anesthesia. After 5 min of irradiation, the right eyes were then instilled with AST (1 mg/ml) and the left eyes instilled with vehicle alone.

Detection of reactive oxygen species (ROS): The eyes were dissected from mice 24 h after UVB exposure and frozen fresh in optimal cutting temperature (OCT) compound with liquid nitrogen. To visualize not only oxidative signaling but also the tissue structure, 4',6-diamidino-2-phenylindole (DAPI) dye (blue) was used to stain the nuclei of the cells. Dihydroethidium (DHE; Sigma-Aldrich, St. Louis, MO), an oxidative fluorescent dye, was used for the immunohistochemical detection of cytosolic superoxide anion (O_2^-) to evaluate ROS production in corneal epithelium tissue, as reported recently [25].

NF-κB immunohistochemistry staining: The eyes were dissected from mice 24 h after UVB exposure and fixed with 4% paraformaldehyde and then paraffin-embedded. To evaluate the NF-κB positive cells in the corneal epithelium, slides were rehydrated and applied with a 1:50 dilution of NF-κB P65 antibody (Santa Cruz Biotechnology, Santa Cruz, CA) for 12 h, washed with PBS and then applied with 1:100 dilution of secondary goat anti–rabbit antibody dye conjugate (Invitrogen, Carlsbad, CA), which gives red fluorescence. Since NF-κB is widely present in intercellular tissue, to detect its expression in cell nuclei, we stained the section slides with 1:100 dilution of YO-PRO®-1 (Invitrogen), which produces a green signal from the cell nuclei. NF-κB positive (yellow) nuclei were quantified in merged images.

In vitro study: TKE2 cells were used for in vitro study. TKE2 is a murine corneal epithelium-derived progenitor cell line [26,27]. Mouse TKE2 cells were cultured in Defined K-SFM (Keratinocye Serum Free Medium) with L-Glutamine, Phenol Red, and Sodium Pyruvate (Invitrogen), supplemented with 100 U/ml of penicillin and 100 U/ml of streptomycin, (Invitrogen). The cells were seeded onto 24-well plates (5×10^4 cells/well) at 37 °C in a humidified incubator containing 5% CO_2. The cells were treated with 1, 0.1, or 0.01 mg/ml AST. After 6 h of incubation, the wells were irradiated with UVB at a dose of 300 mJ/cm^2 at room temperature for 1 min. To prevent UVB radiation absorption, the culture media were removed just before irradiation and replaced with a thin layer of phosphate-buffered saline (PBS). After UVB irradiation, cells were fed with fresh medium. The LDH (lactate dehydrogenase) Cytotoxicity Detection Kit (Roche Applied Science, Penzberg, Germany) was used to determine cytotoxicity 6 h after UVB exposure. Culture supernatants (100 µl) were collected and added to the kit's work solution. After 30 min incubation, the absorbance was measured with an ELISA reader. All procedures were performed according the user manual of the kit. Analysis was performed in triplicate. To determine the background LDH activity of the medium and spontaneous LDH release, additional plates were prepared with empty medium and unaffected cells. The maximum LDH release was achieved by adding 100 µl of Triton-B to the reference wells. Cytotoxicity percentages were calculated, and Triton-B treated wells with

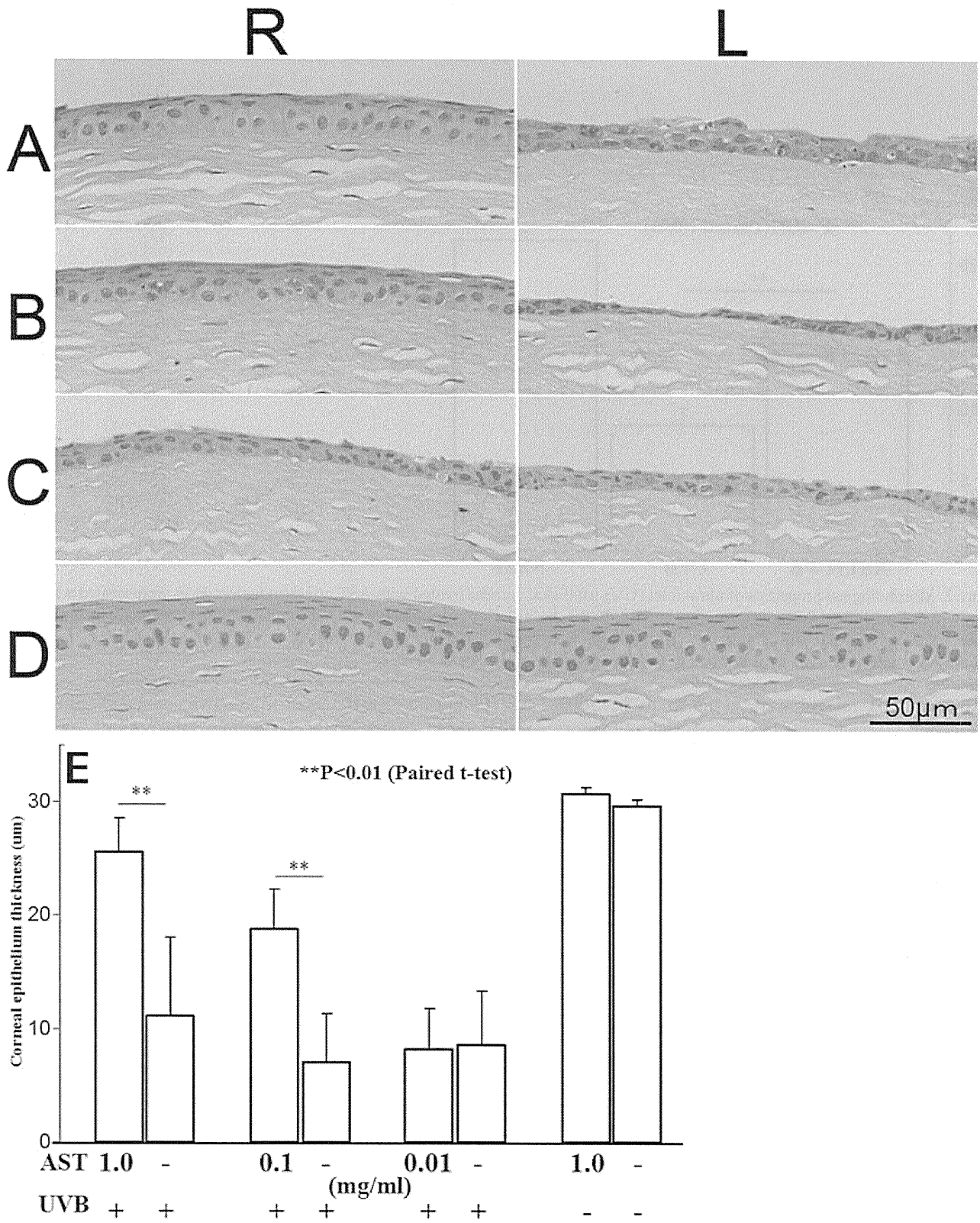

Figure 1. Morphological properties of ultraviolet (UV)-irradiated corneas. Eyes were treated with AST eye drops before UV exposure (**A**: 1 mg/ml, **B**: 0.1 mg/ml, **C**: 0.01 mg/ml AST). Control subjects were not irradiated with UVB (**D**). R: Right eyes were given various concentrations of AST eye drops. L: Left eyes were given vehicle alone as controls. The mean values of corneal epithelial thickness are summarized (E). Epithelia were significantly thicker in right eyes treated with 1 and 0.1 mg/ml AST compared to the left eyes, which served as controls ($p<0.01$). Protective effects of AST were found to occur in a dose-dependent manner.

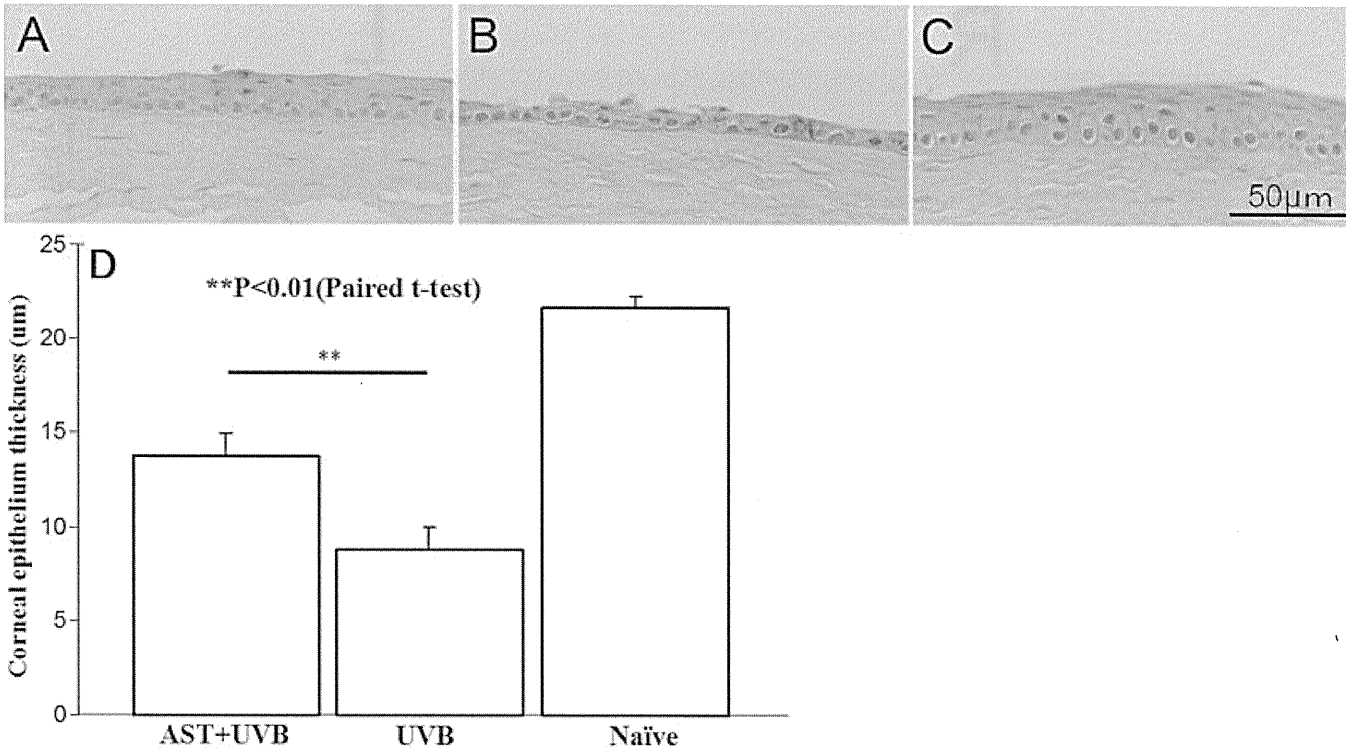

Figure 2. Morphological properties of ultraviolet (UV)-irradiated corneas treated with AST after irradiation. Eyes were treated with AST eye drops within 5 min after UVB exposure (**A**: 1 mg/ml, **B**: 0.1 mg/ml). Control subjects were not irradiated with UVB (**C**). The mean values of corneal epithelial thickness are summarized (**D**). Epithelia were significantly thicker when treated with 1 mg/ml AST compared to fellow eyes as controls ($p<0.01$). The protective effects of AST remained, even if eyes were treated after irradiation.

maximum LDH release were assumed to be 100%. All experiments were performed in triplicate with 5 or more wells for each group in each experiment.

Statistical analysis: All data were expressed as the mean ±standard deviation (SD) from the respective test or control groups of data. Statistical significances were determined by the paired *t*-test and non-parametric Mann–Whitney U-test. P values less than 0.05 were considered significant.

RESULTS

Morphological properties: We examined the morphological properties of UVB-irradiated and control corneas using H&E staining. At 24 h after UVB irradiation at a dose of 400 mJ/cm^2, thinning and ulceration of the corneal epithelial layer were observed (Figure 1). The corneal epithelial thicknesses were 25.6±2.9, 18.8±3.5, and 8.2±3.6 μm in eyes treated with 1, 0.1, and 0.01 mg/ml of AST, respectively. The mean corneal epithelial thickness in eyes untreated with AST was 8.91±5.3 μm after UVB-exposure. The mean corneal epithelium thickness of non-irradiated eyes was 29.6±0.5 μm. Corneal epithelium was well preserved, and the thickness of the epithelium remained close to normal in the right eyes treated with 1 mg/ml of AST instillation (Figure 1A). Its protective effect decreased gradually in a concentration-dependent manner (Figure 1B,C). The corneas of mice administered with AST without UVB irradiation (Figure 1D) showed no differences from naïve corneas (Figure 1D). The mean values of the epithelium thickness of corneas were calculated and summarized (Figure 1E). Corneal epithelia were significantly thicker in eyes treated with 1 and 0.1 mg/ml AST eye drops compared with vehicle-treated eyes ($p<0.01$). Irradiated corneas treated with 1 mg/ml AST showed corneal epithelium thickness close to naïve cornea. AST protected corneal epithelium in a dose-dependent manner (Figure 1E).

We also examined the morphological properties of UVB-irradiated and control corneas using H&E staining when AST was applied to corneas at a concentration of 1 mg/ml 5 min after UVB irradiation at a dose of 400 mJ/cm^2. Twenty-four hours later, the corneal epithelial thickness was 13.7±0.8 μm (Figure 2A). The mean corneal epithelial thickness of vehicle-given corneas was 8.7±1.1 μm after UVB-exposure (Figure 2B). Non-irradiated corneal epithelium was 21.6±0.6 μm thick (Figure 2C). Even when AST was administered after UVB irradiation, the corneal epithelium was significantly thicker than in fellow eyes treated with vehicle ($p<0.01$, Figure 2D).

TUNEL staining: We compared TUNEL staining in the corneas of AST-treated and untreated eyes of the mice 24 h after UV exposure. Few TUNEL-positive nuclei were detected in corneas of mice treated with AST at 1 and 0.1 mg/ml compared to untreated mice after UV irradiation (Figure

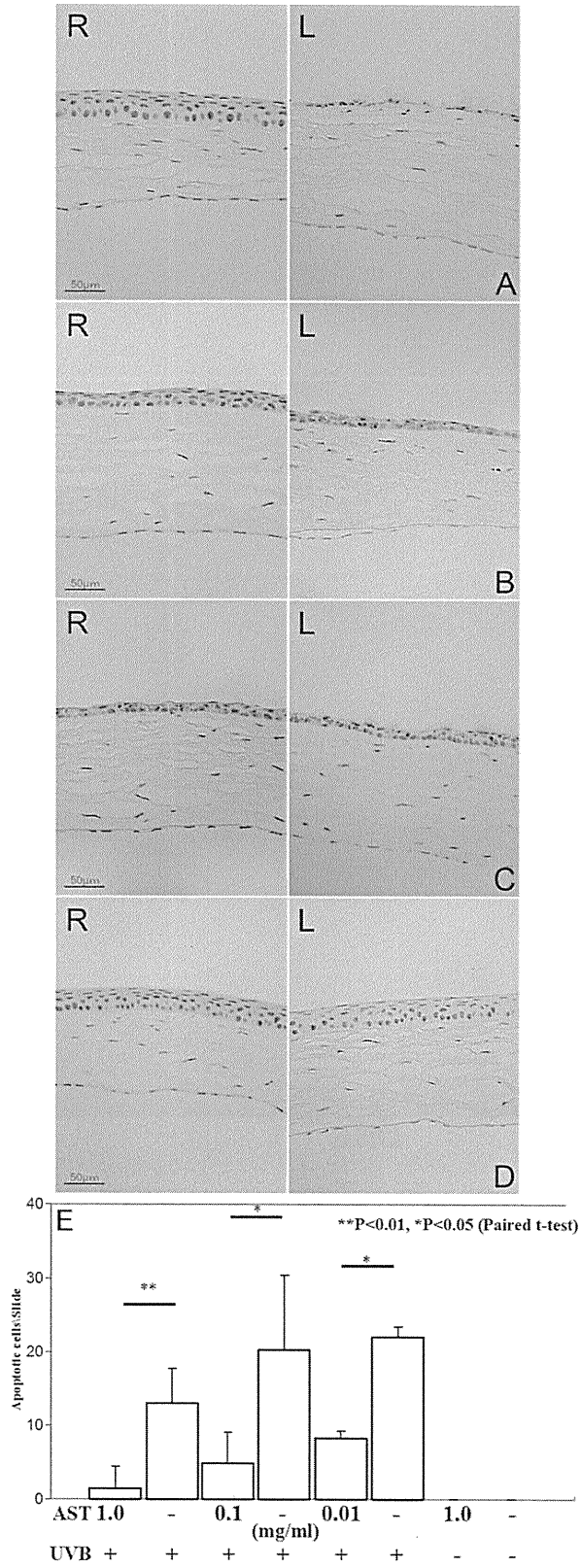

Figure 3. TUNEL labeling at irradiated corneas with and without AST-treatment. Eyes were treated with AST eye drops before UV exposure (**A**: 1 mg/ml, **B**: 0.1 mg/ml, **C**: 0.01 mg/ml AST). Control subjects were not irradiated with UVB (**D**). R: Right eyes were given various concentrations of AST eye drops. L: Left eyes were given vehicle alone as controls. Numbers of apoptotic corneal cells per slide after UVB exposure is shown (**E**). Apoptotic cells were significantly fewer in right eye corneas treated with 1 ($p<0.01$), 0.1 ($p<0.05$), and 0.01 ($p<0.05$) mg/ml AST eye drops compared to the left eyes, which served as controls. There were no apoptotic cells detected in corneas without irradiation.

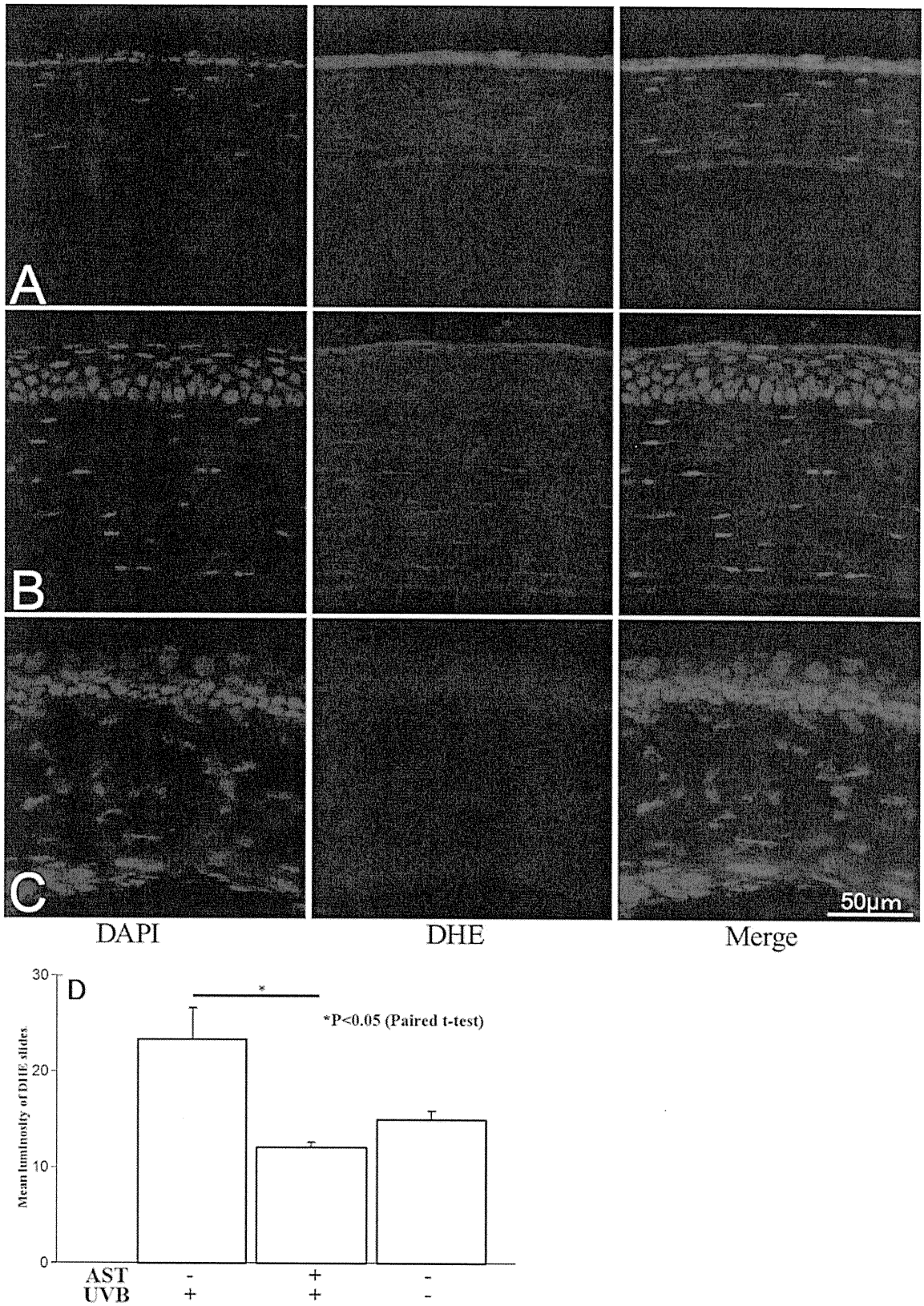

Figure 4. Reactive oxygen species signal expression after UVB exposure. Reactive oxygen species (ROS) were strongly detected (red) in untreated corneal epithelium after UVB irradiation (**A**). The ROS signal was weak in AST treated corneas (**B**) and close to unspecific ROS signaling in naïve corneas (**C**). The mean gray values of the corneal epithelium of DHE stained slides were evaluated by Image J software and summarized (**D**). Mean gray values were significantly lower in corneas treated with 1 mg/ml AST eye drops than in the vehicle-treated eyes ($p<0.05$).

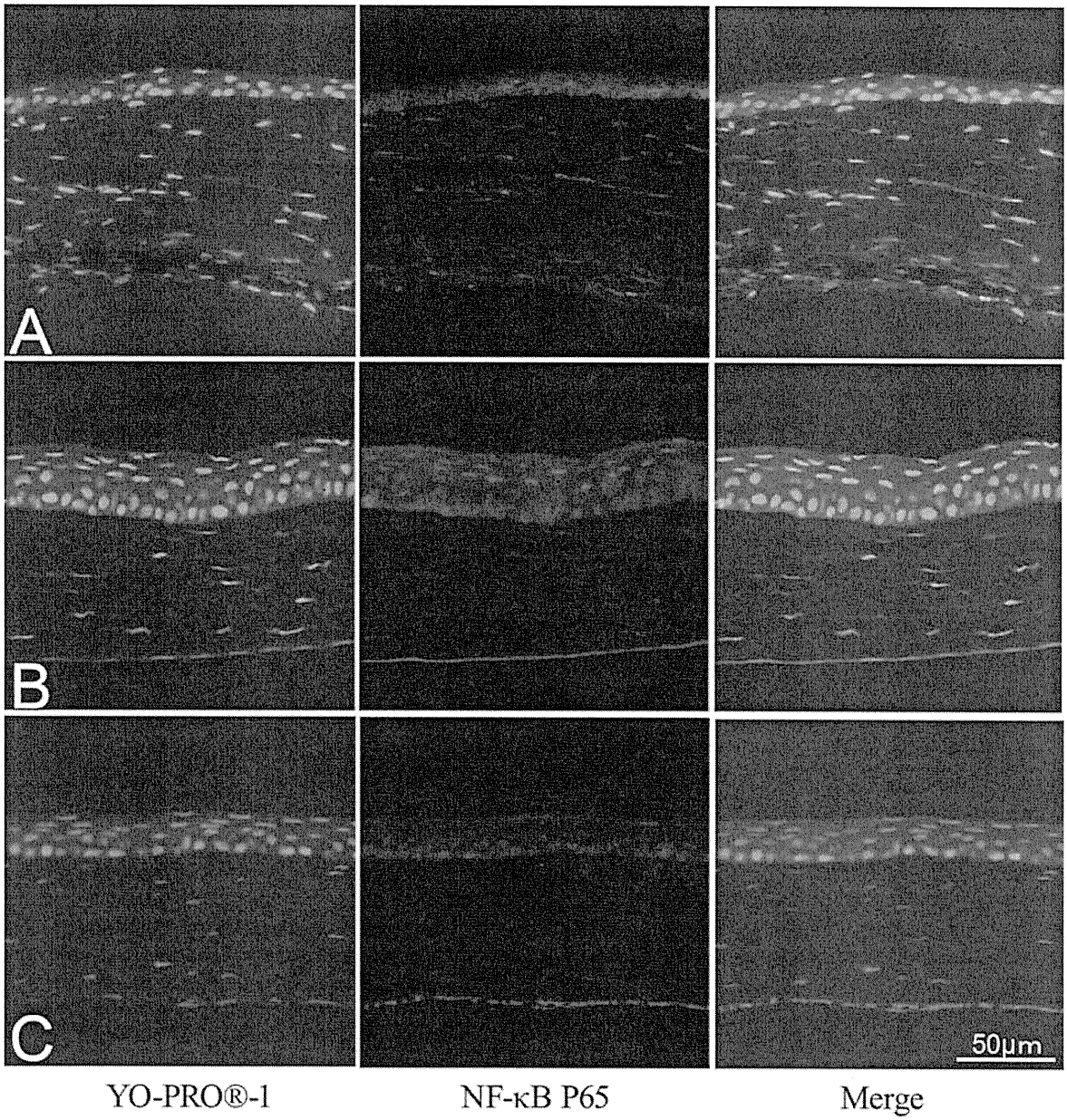

Figure 5. NF-κB expression in corneal epithelia. Eyes were given vehicle alone (**A**) or treated with AST eye drops before UV exposure (**B**); control subjects were not irradiated with UVB (**C**). The mean values of NF-κB positive cells (yellow) in corneal epithelial were summarized (**D**). Expression of NF-κB was significantly downregulated in AST-treated mice after UVB irradiation ($p<0.05$).

3A,B). No significant protective effect was observed in eyes treated with AST 0.01 mg/ml (Figure 3C). There were no apoptotic cells detected in corneas without UVB exposure (Figure 3D).

TUNEL-positive cells were counted, and the numbers were 1.5±3.0, 5.0±4.1, and 8.25±0.9 in eyes treated with 1, 0.1, and 0.01 mg/ml of AST, respectively (Figure 3E). The mean number of apoptotic cells was 18.4±4.7 in vehicle-given irradiated corneas. The apoptotic cells were significantly fewer in corneas treated with AST than those with vehicle only ($p<0.01$).

Detection of reactive oxygen species (ROS): Confocal microscopic images was examined to quantify reactive oxygen species (ROS) production in mouse corneal tissue. ROS production was determined by conversion of DHE to ethidium bromide (EtBr). All images were made in parallel at identical settings (Figure 4). ROS were strongly detected in untreated corneal epithelium after UVB irradiation (Figure 4A). However, the ROS signal was downregulated in AST-treated corneas (Figure 4B) and close to unspecific ROS signaling in naïve corneas (Figure 4C). The mean gray values of the corneal epithelium of DHE stained slides were evaluated by Image J software and summarized in Figure 4D. The mean gray value in vehicle-given irradiated corneas was 23.3±3.3. In eyes treated with 1 mg/ml of AST, after UVB irradiation, the mean gray value was 12.08±0.5. Non-irradiated corneal epithelium showed a 15.04±0.8 mean gray value. AST-treated epithelium showed significantly ($p<0.05$) lower mean gray values than irradiated corneas did.

NF-κB downregulation by AST: Previously, we reported that AST decreased NF-κB expression in endotoxin-induced uveitis (EIU) and choroidal neovascularization [23,24]. To examine whether AST administration effects NF-κB in corneal epithelium, we immunohistochemically analyzed AST expression in the collected corneal tissues and examined it with confocal microscope. NF-κB positive nuclei (yellow) were found to be 13.0±7.9 in corneal epithelial cells in UV-irradiated mice treated with AST at 1.0 mg/kg (Figure 5A). However, 36.0±6.2 (Figure 5B) of multiple NF-κB positive cells were found in the corneal epithelial cells in UV-irradiated mice untreated with AST. Naïve mice corneal tissues showed weak response to anti-NF-κB antibodies, and only 1.3±1.1 positive nuclei were found (Figure 5C). Expression of NF-κB was significantly downregulated in AST-treated mice after UVB irradiation ($p<0.05$, Figure 5D).

AST suppressed phototoxicity in corneal epithelial cell cultures after UVB irradiation: Next, cytotoxicity was examined in UVB-irradiated TKE2 cells, murine corneal epithelium-derived progenitor cell line, treated or untreated with AST in vitro (Figure 6). The percentages of cytotoxicity after irradiation were 17.6±2.0, 29.5±2.2, 31.7.2±2.8, and 32.7±1.7% in wells containing 1, 0.1, 0.01, and 0 mg/ml of AST, respectively. Cytotoxicity was significantly suppressed by 1 mg/ml ($p<0.01$) and 0.1 mg/ml ($p<0.05$) AST administration. The effect was AST concentration-dependent.

DISCUSSION

The corneal epithelium serves to protect corneal structures against UV damage by absorbing a substantial amount of UV energy. Though the energy of UV is much less than that of ionizing radiation rays, the injuries on cells and DNA are critical. Excessive UVB irradiation induces various changes of DNA, proteins and cells, through activation of pro-inflammatory mediators including NF-κB. AST can form stable resonance structures by attachment of the carbonyl and hydroxyl groups to its β-ionone ring. It can also remove the chain-carrying lipid peroxyl radicals in the liposomal suspension, protecting cells from oxidative and free radical damages. NF-κB activates proinflammatory cytokines, chemokines, and enzymes that generate mediators of inflammation. It can also activate adhesion molecules that play a key role in the initial recruitment of leukocytes to sites of inflammation. Therefore, activation of NF-κB leads to a coordinated upregulation of many genes whose products mediate the inflammatory loop and perpetuate local inflammatory responses. In our previous studies, AST inhibited the in vivo activation of NF-κB in endotoxin-induced uveitis (EIU) and choroidal neovascularization [23, 24]. Therefore, reactive oxygen species-induced oxidative stress may play an important role in NF-κB activation and proinflammatory cytokine production. Our immunohistochemical finding shows that AST has the same effects of reducing NF-κB expression in corneal epithelia. The anti-inflammatory effects of AST, through its suppression of NF-κB activation, may be based on its antioxidant activity,

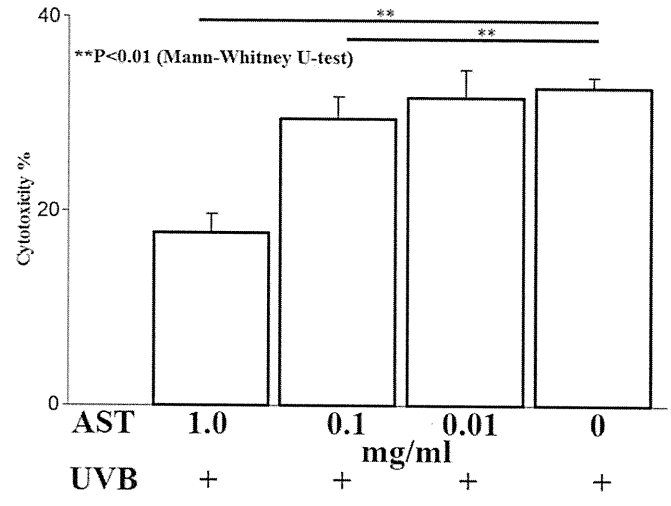

Figure 6. UVB-induced cytotoxicity in TKE2 cells in vitro. AST was added to a culture of UVB-irradiated TKE2 cells. Cytotoxicity after UVB exposure in keratinocyte cultures was significantly decreased by AST in a dose-dependent manner (1 mg/ml: $p<0.01$, 0.1 mg/ml: $p<0.05$, and 0.01 mg/ml: not significant).

as previous reports showed that several antioxidants efficiently inhibit NF-κB activation induced by lipopolysaccharides (LPS) in cell systems [28-33]. Therefore, these effects appear to be mediated by the powerful radical scavenger properties of the antioxidants, which apparently counteract reactive oxygen intermediates generated by NF-κB activation [30,34,35].

We also showed that the relieving effect of AST on UVB photokeratitis is not derived from light-interception (sunglasses effect) but its direct pharmacological effect (Figure 2). In fact, a previous study showed that AST eye drops did not delay the progression of UVB-induced cataract in rats when AST was not on lens [36]. In addition, UVB irradiation improved AST accumulation in green microalgae [8]. These results strongly suggest that AST can produce a protective effect against UV, and organisms have been using AST to save themselves from harmful UV light.

AST is found abundantly in the red-orange pigment of marine animals such as salmon (and salmon roe) and the shells of crabs and shrimp. Humans have taken in these food products since ancient times, and AST is now available as an oral supplement. Therefore, AST may be free of any harmful side effects. In the present study, we demonstrated that topical AST, instead of systemic administration, is effective in protecting the ocular surface against UV exposure with no adverse effects. Thus, in conclusion, AST might be a promising naturally-derived substance for protecting ocular surfaces from the damages caused by ultraviolet radiation.

ACKNOWLEDGMENTS

This work was supported by grants from the Japan Society for the Promotion of Science (JSPS); the Ministry of Education, Culture, Sports, Science, and Technology (MEXT); and the Mishima Memorial Foundation, Japan.

REFERENCES

1. Schein OD. Phototoxicity and the cornea. J Natl Med Assoc 1992; 84:579-83. [PMID: 1629921]
2. Cullen AP, Chou BR, Hall MG, Jany SE. Ultraviolet-B damages corneal endothelium. Am J Optom Physiol Opt 1984; 61:473-8. [PMID: 6465280]
3. Kitaichi N, Shimizu T, Yoshida K, Honda A, Yoshihisa Y, Kase S, Ohgami K, Norisugi O, Makino T, Nishihira J, Yamagishi S, Ohno S. Macrophage migration inhibitory factor ameliorates UV-induced photokeratitis in mice. Exp Eye Res 2008; 86:929-35. [PMID: 18436209]
4. Suzuki Y, Ohgami K, Shiratori K, Jin XH, Ilieva I, Koyama Y, Yazawa K, Yoshida K, Kase S, Ohno S. Suppressive effects of astaxanthin against rat endotoxin-induced uveitis by inhibiting the NF-kappaB signaling pathway. Exp Eye Res 2006; 82:275-81. [PMID: 16126197]
5. Moreira AJ, Fraga C, Alonso M, Collado PS, Zetller C, Marroni C, Marroni N, Gonzalez-Gallego J. Quercetin prevents oxidative stress and NF-kappaB activation in gastric mucosa of portal hypertensive rats. Biochem Pharmacol 2004; 68:1939-46. [PMID: 15476665]
6. Clark RA, Valente AJ. Nuclear factor kappa B activation by NADPH oxidases. Mech Ageing Dev 2004; 125:799-810. [PMID: 15541774]
7. Shao DZ, Lee JJ, Huang WT, Liao JF, Lin MT. Inhibition of nuclear factor-kappa B prevents staphylococcal enterotoxin A-induced fever. Mol Cell Biochem 2004; 262:177-85. [PMID: 15532722]
8. Woo SH, Park IC, Park MJ, An S, Lee HC, Jin HO, Park SA, Cho H, Lee SJ, Gwak HS, Hong YJ, Hong SI, Rhee CH. Arsenic trioxide sensitizes CD95/Fas-induced apoptosis through ROS-mediated upregulation of CD95/Fas by NF-kappaB activation. Int J Cancer 2004; 112:596-606. [PMID: 15382040]
9. Ohta K, Nakayama K, Kurokawa T, Kikuchi T, Yoshimura N. Inhibitory effects of pyrrolidine dithiocarbamate on endotoxin-induced uveitis in Lewis rats. Invest Ophthalmol Vis Sci 2002; 43:744-50. [PMID: 11867593]
10. Fassett RG, Coombes JS. Astaxanthin, oxidative stress, inflammation and cardiovascular disease. Future Cardiol 2009; 5:333-42. [PMID: 19656058]
11. Jyonouchi H, Sun S, Tomita Y, Gross MD. Astaxanthin, a carotenoid without vitamin A activity, augments antibody responses in cultures including T-helper cell clones and suboptimal doses of antigen. J Nutr 1995; 125:2483-92. [PMID: 7562082]
12. Kobayashi M. In vivo antioxidant role of astaxanthin under oxidative stress in the green alga Haematococcus pluvialis. Appl Microbiol Biotechnol 2000; 54:550-5. [PMID: 11092631]
13. Spiller GA, Dewell A. Safety of an astaxanthin-rich Haematococcus pluvialis algal extract: a randomized clinical trial. J Med Food 2003; 6:51-6. [PMID: 12804020]
14. Chew BP, Park JS, Wong MW, Wong TS. A comparison of the anticancer activities of dietary beta-carotene, canthaxanthin and astaxanthin in mice in vivo. Anticancer Res 1999; 19:1849-53. [PMID: 10470126]
15. Ikeuchi M, Koyama T, Takahashi J, Yazawa K. Effects of astaxanthin in obese mice fed a high-fat diet. Biosci Biotechnol Biochem 2007; 71:893-9. [PMID: 17420580]
16. Pashkow FJ, Watumull DG, Campbell CL. Astaxanthin: a novel potential treatment for oxidative stress and inflammation in cardiovascular disease. Am J Cardiol 2008; 101:58D-68D. [PMID: 18474276]
17. Choi SK, Park YS, Choi DK, Chang HI. Effects of astaxanthin on the production of NO and the expression of COX-2 and iNOS in LPS-stimulated BV2 microglial cells. J Microbiol Biotechnol 2008; 18:1990-6. [PMID: 19131704]
18. Barrow CJ, Shahidi F. Marine nutraceuticals and functional foods. Boca Raton: CRC Press; 2008.
19. Liu X, Shibata T, Hisaka S, Osawa T. Astaxanthin inhibits reactive oxygen species-mediated cellular toxicity in dopaminergic SH-SY5Y cells via mitochondria-targeted protective mechanism. Brain Res 2009; 1254:18-27. [PMID: 19101523]
20. Kurashige M, Okimasu E, Inoue M, Utsumi K. Inhibition of oxidative injury of biological membranes by astaxanthin. Physiol Chem Phys Med NMR 1990; 22:27-38. [PMID: 2084711]
21. Bennedsen M, Wang X, Willen R, Wadstrom T, Andersen LP. Treatment of H. pylori infected mice with antioxidant